To the Graduate Council:

I am submitting herewith a dissertation written by Aldo Durazzo entitled "Exsolution in the Systems Bornite-Chalcopyrite and Pyrrhotite-Pentlandite: An Approach to Textural Interpretation." I recommend that it be accepted in partial fulfillment of the requirements for the degree of Doctor of Philosophy, with a major in Geology.

Lawrence A. Taylor
Lawrence A. Taylor, Major Professor

We have read this dissertation
and recommend its acceptance:

Krola C. Misra

Leo F. Oliveri

Otto C. Kopp

John B. Higgins

Accepted for the Council:

L Evans Roth
Vice Chancellor
Graduate Studies and Research

EXSOLUTION IN THE SYSTEMS BORNITE-CHALCOPYRITE AND PYRRHOTITE-PENTLANDITE: AN APPROACH TO TEXTURAL INTERPRETATION

A Dissertation

Presented for the

Doctor of Philosophy

Degree

The University of Tennessee, Knoxville

Aldo Durazzo

August 1980

ACKNOWLEDGMENTS

My most sincere thanks are conveyed to Dr. Lawrence A. Taylor, who served as major advisor for this dissertation and provided the encouragement and support which made the present investigation possible.

The members of the committee, Dr. Kula C. Misra, Dr. Otto C. Kopp, and Dr. Ben F. Oliver, gave both constructive criticism and valuable suggestions, which were essential for improving the manuscript. In addition, Dr. Misra made available natural ore samples from The University of Tennessee Department of Geological Sciences. A special thank you is extended to Robin Brett of the National Science Foundation, who kindly helped in the revision of the first chapter of the manuscript, for his advice and encouragement.

Finally, the assistance and support of my wife Mary are warmly acknowledged.

This research was partially funded by grants from the Geological Society of America, the Don Jones Fund of The University of Tennessee, and the Exxon Corporation.

ABSTRACT

Textural interpretation of natural bornite-chalcopyrite (bn-cpy) and pyrrhotite-pentlandite (po-pn) intergrowths was attempted by performing exsolution and coarsening experiments in sealed, evacuated silica tubes. Bn-cpy solid solutions and monosulfide solid solutions (mss) of various compositions were synthesized and annealed between 20 minutes and 10 weeks at temperatures between 250° and 100° C and 400° and 200° C respectively. The resulting exsolution textures, consisting of cpy bodies in bn and pn bodies in mss, were related to composition, annealing temperature, and annealing time. Their establishment and evolution were described by T-T-T (isopleth) and isochronous diagrams.

The development of early textural forms occurs through nucleation and growth and is marginally affected by coarsening of the exsolution products. Therefore, the initial degree of supersaturation and the values of the diffusivities, both of which are functions of the temperature, determine the early textural features of the experimental charges. The final textures derive from further growth of the early forms but may also involve substantial coarsening and spheroidization above certain temperatures. Therefore, textural features may serve as geothermometers.

Coarsening experiments on cpy lamellar forms and cooling experiments on homogeneous mss of various compositions were also performed. The experimental results of this study indicate that bn-cpy

mutual boundary textures form above about 250° C and, therefore, are compatible with:

1. Simultaneous precipitation of bn and cpy;
2. Exsolution during slow cooling from temperatures above the solvus;
3. Metamorphism to temperatures in excess of about 250° C.

Widmanstätten textures involving bn-cpy are not easily explained by slow cooling, but indicate:

1. Low-temperature replacement; or
2. Exsolution of cpy lamellae from anomalous bornites during mild metamorphism (i.e., heating to temperatures not exceeding 200°-250° C).

Massive pn in po develops by exsolution during slow cooling from temperatures above the solvus, in the 250°-610° C temperature range. Pentlandite bodies oriented along one direction in the matrix are compatible with exsolution at temperatures between about 150° and 250° C. Pentlandite flames form by exsolution at or below 150° C. Widmanstätten textures consisting of pn lamellae in mss—obtained experimentally under high degrees of supersaturation—cannot form by exsolution by slow cooling.

TABLE OF CONTENTS

LIST OF TABLES

LIST OF FIGURES

FIGURE PAGE

FIGURE PAGE

CHAPTER I

INTRODUCTION

The study of textural features has long been considered a potentially useful approach in reconstructing the genetic history of rocks, including those of sulfide mineral deposits. Microscopic observation of mineral assemblages helps in the reconstruction of the paragenetic sequence of a deposit, and in the establishment of whether simultaneous formation, replacement, or recrystallization of given mineral species has occurred (e.g., Van der Veen, 1925). Experimental studies are also useful, since they may allow given textural features, obtained under controlled conditions, to be related to processes such as exsolution (Schwartz, 1931b) or replacement (Schouten, 1934). In the majority of cases, however, the meaning of textures has not been fully understood (Barton, 1970).

A major difficulty in attempting textural interpretations is that, while given physico-chemical conditions during ore genesis produce characteristic textures, a number of textures can be obtained experimentally by more than one process (Schouten, 1934; Brett, 1964; Ramdohr, 1969). As a result, a meaningful analysis of cause-effect relationships of mineral assemblages appears to be far from simple. The complexities involved are reflected by the relatively large number of textural classifications which have come into existence. Those based on geometric criteria are merely descriptive (e.g., Ramdohr, 1969); others are based on genetic as well as geometric criteria, and

inevitably lead to controversy (e.g., Bastin, 1931; Schwartz, 1951; Edwards, 1954; Ramdohr, 1969).

One of the potentially most rewarding uses of textural analysis is in geothermometry (e.g., Edwards, 1954). The majority of sulfide mineral assemblages reflect equilibrium conditions not far removed from 25° C, owing to the rapid reaction kinetics associated with their establishment (Barton and Skinner, 1967). Consequently, the applicability of most sulfide coexisting-phase and sliding-bar geothermometers is questionable (Brett, 1962; Barton and Skinner, 1967; Taylor, 1971). However, textural configurations established during the achievement of chemical equilibrium, which involve nucleation and growth, may also be affected by grain coarsening and spheroidization.[1] The latter processes strongly depend on the diffusivities of the atoms present, and therefore on the temperature, and may take place independently of chemical re-equilibration. Accordingly, original sulfide textures can be modified depending on whether or not further growth and/or coarsening takes place. The experimental determination of temperatures below which pre-existing textural features are not erased can be used in geothermemetry.

The importance of temperature in the establishment and evolution of ore mineral textures is particularly evident in systems in

---

[1] This may be defined as an extreme form of coarsening, whereby exsolved bodies tend to assume a spherical shape.

which the phases present form solid solutions at high temperature and separate out at low temperature through exsolution.[2]

In the present investigation, two mineral pairs were selected, which form solid solutions at high temperature, and unmix at low temperature, i.e., bornite-chalcopyrite (bn-cpy) and pyrrhotite-pentlandite (po-pn). Their natural intergrowths often resemble the intergrowths obtained in the laboratory by exsolution (Figures 1.1, 1.2, 1.3, 1.4). Therefore, the meaning of some bn-cpy and po-pn natural intergrowths can be better understood if they are compared to exsolution textures obtained experimentally under controlled conditions.

Some uncertainty is involved in this approach since exsolution need not be the only process producing the natural textures relevant to this study. Replacement, for instance, may produce practically identical textures, and morphologic criteria to distinguish exsolution from replacement intergrowths are not entirely satisfactory (e.g., Schouten, 1934; Ramdohr, 1969). However, in the opinion of many (e.g., Van der Veen, 1925; Naldrett et al., 1967; Ramdohr, 1969), a substantial portion of the natural intergrowths of bn-cpy and po-pn are the result of exsolution.

The purpose of the present study was:

1. To assess how physico-chemical factors such as temperature, composition, and time affect the formation and development of bn-cpy and po-pn exsolution textures.

---

[2]Exsolution is defined as "the process of isochemical separation of one or more phases from an originally homogeneous phase without the complete disappearance of the original phase" (Barton, 1972).

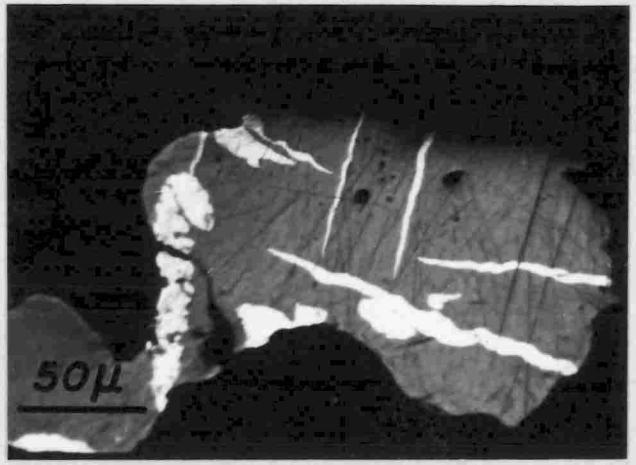

Figure 1.1. Mutual boundary and lamellar texture; Butte, Mont. (gray: bn; white: cpy).

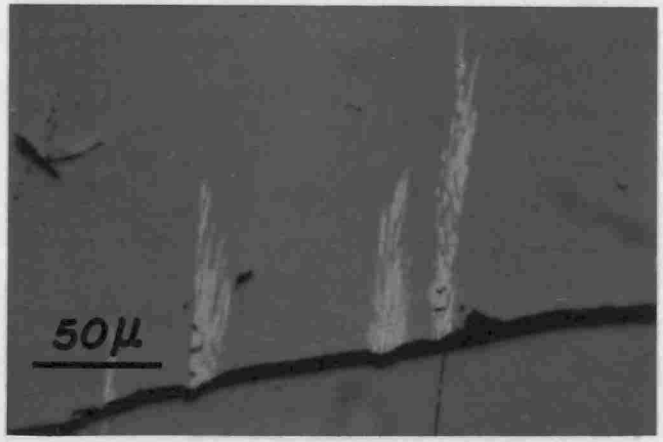

Figure 1.3. Flame texture; Sudbury, Ont. (gray: po; white: pn).

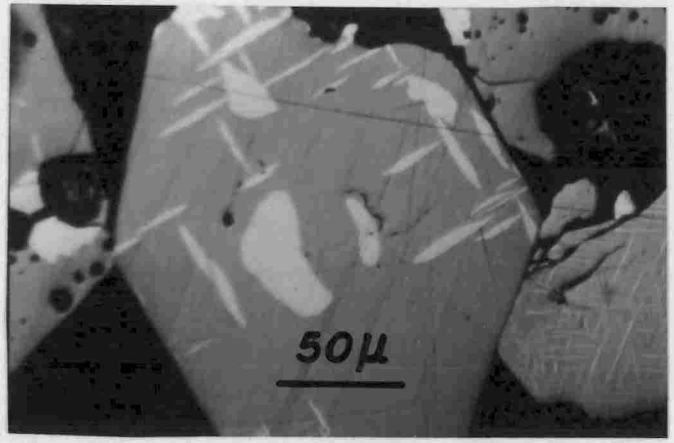

Figure 1.2. Widmanstätten lamellae and patches; the small grain shows a pervasive Widmanstätten texture; 30% cpy charge annealed 1 week at 150° C and 4 weeks at 300° C (gray: bn; white: cpy).

Figure 1.4. Flame texture; 20% Ni, 37.5% S charge cooled from 500° to 100° C at 1° C/hour (gray: mss; white: pn).

2. To interpret, on the basis of the experimental results, some of the natural textures formed by these minerals, the bn-cpy and po-pn intergrowths.

CHAPTER II

THE KINETICS OF EXSOLUTION INVOLVING BORNITE-CHALCOPYRITE AND THEIR BEARING ON THE INTERPRETATION OF NATURAL BN-CPY TEXTURES

A. INTRODUCTION

Bornite-chalcopyrite (bn-cpy) intergrowths are common in many copper mineral deposits. In theory, these intergrowths may originate in three ways: (1) by simultaneous precipitation of the two phases; (2) by exsolution; and (3) by replacement. The first of these processes is inferred from the phase relations within the Cu-Fe-S ternary system (Kullerud et al., 1969) and the bn-cpy pseudo-binary system (Sugaki, 1965). It involves eutectic crystallization of bn solid solution and intermediate solid solution (iss) at temperatures in excess of about 830° C, followed by various re-equilibration steps (Sugaki, 1965; Cabri, 1973). Co-precipitation of bn and cpy from aqueous solution has also been suggested on the basis of experimental evidence (Roberts, 1963).

Exsolution, with which this paper is concerned, has been widely investigated experimentally in connection with textural interpretation. Replacement has been observed in nature (e.g., Ramdohr, 1969) and produced in the laboratory (Ray, 1930; Schouten, 1934). Its importance in connection with textural studies is briefly analyzed in a later section.

The present study was undertaken in order to better understand the meaning of textures commonly observed in bn-cpy intergrowths, particularly in connection with the thermal history of the deposits in which they are contained. More specifically, the analysis was concerned with the kinetics of cpy[1] exsolution from bn-rich solid solutions along the Cu_5FeS_4-$CuFeS_{1.9}$ join (Figure 2.1) following homogenization at high temperature,[2] and the subsequent kinetics of coarsening.

Some of the annealing experiments of this study were conducted at 100° and 150° C, because it was felt that only at relatively low temperatures can a number of bn-cpy natural textures be established and retained. Experiments at higher temperatures (i.e., between 200° and

---

[1] Cabri (1973) determined that several phases, close in composition and physico-chemical properties to $CuFeS_2$ (i.e., talnakhite, mooihoekite, and haycockite) have often been mistaken for cpy in the past. Their composition and stability are strongly influenced by kinetic factors, and assemblages containing them may not reflect thermodynamic equilibrium (Putnis, 1978). In the present study, no efforts were made to determine which if any of these "cpy-like" phases were involved in the exsolution process; accordingly, the term "cpy" may include any of these phases in addition to $CuFeS_2$.

Some of the present experiments (6 mole % cpy at 100° and 150° C) show very minor occurrences of a bluish phase associated with cpy veinlets or lamellae. They are too small to be analyzed by the electron microprobe (i.e., ≈1 μm across), but probably consist of digenite, whose presence in some portions of the bn-cpy system was observed by Brett below 200° C (1963).

[2] Stoichiometric cpy ($CuFeS_2$) is not stable at temperatures above 550° C (MacLean et al., 1972), and charges with the $Cu_5FeS_4/CuFeS_2$ ratio required for the experiments would not form a homogeneous solid solution at the homogenization temperatures. Accordingly, past experiments involving bn-cpy exsolution (e.g., Brett, 1964; Sugaki, 1965) were conducted on homogeneous charges lying on the Cu_5FeS_4-$CuFeS_{2-x}$ join. A similar approach was adopted in this study.

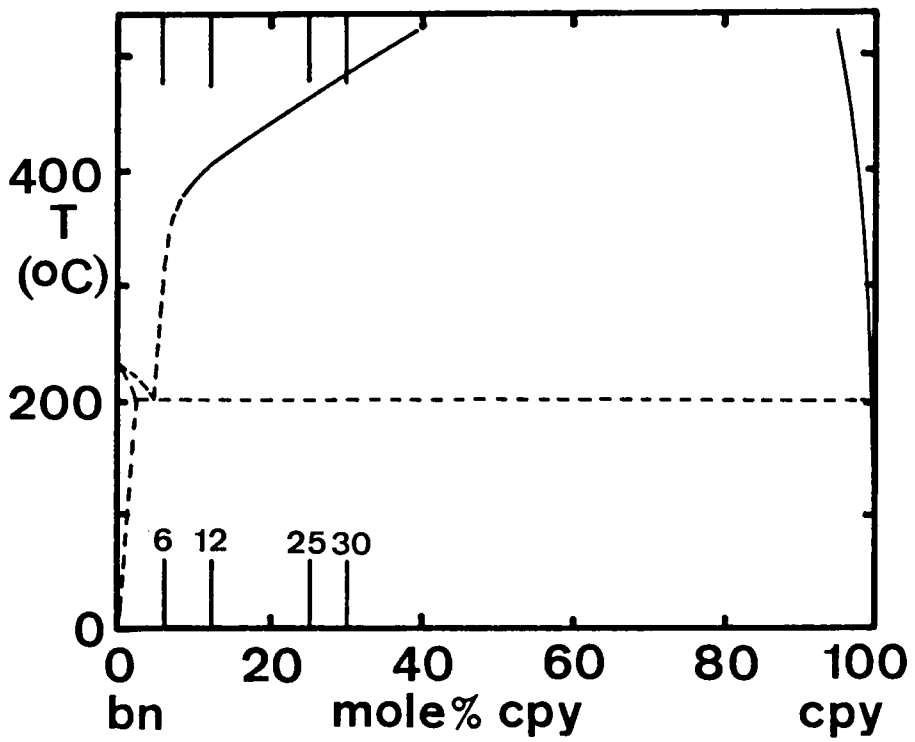

Figure 2.1. Pseudobinary phase diagram, bn-cpy system; adapted from Brett (1963) and Sugaki (1965) (bn: bornite; cpy; chalcopyrite).

350° C) were also performed, to investigate textural development at higher temperatures, and to compare the present results with those obtained by Brett (1964) in his classic textural investigation. In addition, some experiments were conducted on charges containing 500 ppm Se in order to assess the possible influence of minor concentrations of this element on textural development. An account of the preliminary results of this study was given by Durazzo and Taylor (1978).

B. PREVIOUS STUDIES

Following the early work by Schwartz (1931a), experiments were performed in Japan on bn-cpy exsolution (Sugaki, 1951a, 1951b, 1955, 1965; Takeuchi and Nambu, 1956). Brett's classic studies (1962, 1963, 1964) were the first systematic attempts to assess the influence of various thermodynamic, as well as kinetic, factors on the evolution of exsolution textures. His investigation remains the most comprehensive study in this field to date. The studies considered to be most relevant to the present investigation are outlined below.

Schwartz (1931a) homogenized natural bn-cpy intergrowths in nonevacuated pyrex and silica glass tubes above 475° C. On the basis of subsequent cooling experiments, he concluded that the bn-cpy lamellar (Widmanstätten) intergrowths observed in mineral deposits, and thought to have originated by exsolution, formed during extremely rapid cooling from above 475° C. Rapid cooling was considered responsible for the establishment of similar textures by Edwards (1954) and Lyon (1959), also on the basis of experimental evidence.

Sugaki (1951b) performed isothermal experiments on natural bn-cpy intergrowths in sealed, nonevacuated silica-glass tubes, and estimated the homogenization temperature for his charges at between 300° and 350° C. These values are considerably lower than those obtained by Schwartz (1931a), probably because the bulk compositions of the samples considered by the two investigators were different. Subsequently, Sugaki (1951b) performed annealing experiments between 100° and 450° C on samples homogenized at high temperatures. Various textural types, often co-existing in the same charge, resulted. In general, narrow cpy lamellae resulted at the lower annealing temperatures, while coarsened forms prevailed at the higher temperatures. Although a definite relationship emerged between textural types and annealing temperatures, the annealing times of the experiments were limited (i.e., they did not exceed 72 hours). Moreover, a clear dependence of textural features on bulk composition could not be established, since only natural samples of uncertain and probably variable composition were used.

Brett (1962, 1963, 1964) conducted cooling and annealing experiments in evacuated silica-glass tubes, using synthetic materials of various compositions along the bn-cpy join. He obtained a great variety of textures, largely similar to those described by the previous investigators. In addition, he produced textures not normally ascribed to exsolution (e.g., pseudo-replacement and pseudo-veins). Although no clear relationship emerged between textural features and such parameters as temperature and cooling rate, Brett (1964) suggested that the preservation of early-formed crossing lamellae in some

slow-cooling runs is due to the extreme dilution of the original solid solution, which prevents the buildup of excessive strain, thus allowing crystallographic coherency to be maintained at the bn-cpy interfaces.[3] In the case of less diluted solutions, early exsolution, followed by loss of coherency, coarsening, and erasure of the initial lamellar forms, would produce low supersaturation in the matrix and lead, at low temperatures, to the formation of a second generation of lamellae (secondary exsolution). These explanations were offered as an alternative to Schwartz's suggestion (1931a) that lamellae can only be formed and retained by rapid cooling.

Despite the validity of the experimental approach used by Brett (1964), no systematic annealing experiments were conducted below 200° C. Cooling runs to 50° C, on the other hand, revealed textural features acquired largely at high temperature.

C. EXPERIMENTAL PROCEDURE

Bornite solid solution members (Table 2.1 and Figure 2.1) were synthesized in sealed, evacuated silica-glass tubes using high-purity elements, according to the techniques described by Kullerud (1971). Before synthesis, Fe sponge (Johnson Matthey Chemical Ltd., grade 1, 99.998% spec. pure) was reduced in a hydrogen stream at 900% C for over

---

[3]Coherency implies crystallographic continuity across the interface separating the matrix from the precipitate, and requires parallel orientation as well as equal spacing in both structures. When these conditions are only partly met, semicoherency is achieved. Total mismatch results in incoherency.

Table 2.1

Composition of Stoichiometric Bornite and of the Experimental Charges Used in the Present Study

Mole %		Atomic %			Weight %		
Cu_5FeS_4	$CuFeS_{1.9}$	Cu	Fe	S	Cu	Fe	S
100	0	50.00	10.00	40.00	63.31	11.13	25.56
94	6	49.41	10.38	40.21	62.68	11.58	25.74
88	12	48.77	10.79	40.44	62.00	12.06	25.94
75	25	47.20	11.80	41.00	60.53	13.30	26.17
70	30[a]	46.51	12.24	41.25	59.56	13.78	26.66

[a]For this composition, quenching in cold water from 600°, 700°, and 800° C produced Widmanstätten lamellae in the bornite solid solution.

2 hours, to eliminate any trace of oxides. Fresh Cu filings were obtained from ASARCO Cu rod (99.999+% spec. pure). Sulfur and Se (both 99.999+%) were also from ASARCO.

In order to obtain homogeneous products, the charges were annealed at 700° C for 1 week and quenched in water. Their content was subsequently ground in a diamonite mortar under toluene to a particle size of about 0.2 mm, sealed in new tubes under vacuum, and annealed at 700° C for an additional 2-3 weeks. In some instances, this procedure had to be repeated 1-2 times. Homogeneity and composition were checked by optical examination in reflected light, electron microprobe analysis, and x-ray powder diffraction. It was not possible to ascertain the size of the individual bn solid solution grains within each aggregate particle at this stage: even etching proved unsuccessful.

Individual charges weighing about 20 mg were subsequently annealed at temperatures between 250° and 100° C, for times ranging between 20 minutes and 10 weeks, quenched in cold water, and examined optically and by x-ray diffractometry (Appendix A). In some cases, electron microprobe analyses were performed using a fully-automated MAC 400 S instrument, operating at 15 kV, with a beam current of 0.03 μA, spot diameter of 1-2 μm. Metallic copper and troilite, or synthetic bornite, were used as standards. Corrections for matrix effects were applied according to procedures described by Ziebold and Ogilvie (1963).

D. PRESENTATION OF RESULTS AND DISCUSSION

Textural Terminology

The textural forms obtained from the isothermal experiments are conveniently grouped into "early types" and "mature types." The former are observed after short annealing times (i.e., few minutes to few hours depending on the annealing temperature) and seldom exceed 1-2 μm in width. The latter result from growth and coarsening of the early types after annealing times ranging between several hours and several days, and are usually larger than 3 μm across. The terminology used to describe these textures has been adapted from that commonly used in the ore microscopy literature (e.g., Van der Veen, 1925; Edwards, 1954; Ramdohr, 1969). Some textural terms have been given different meanings by different authors, or have been loosely defined. In order to avoid confusion, all applicable terms are redefined and illustrated below.

The early types, whose symbol consists of one letter only, include:

Cell (C, Hawley, 1962), also referred to as "network" (Van der Veen, 1925): cpy occurrences along grain boundaries or cracks, appearing as continuous or discontinuous veinlets within the matrix (Figures 2.2 and 2.3).

Patches (P: irregular cpy bodies tending to assume an equant shape around holes, cracks, and grain boundaries (Figure 2.4).

Widmanstätten (W, Schwartz, 1931b); also referred to as "lattice" (Van der Veen, 1925); "crystallographic" (Schwartz, 1931b); "lamellar" (Ramdohr, 1969): thin blades or lamellae developed along

two or more directions in the bn matrix. They are often similar to the Widmanstätten patterns of kamacite/taenite observed in iron meteorites (Figures 2.2, 2.5, 2.6).

The mature types, for which two-letter symbols are used, include:

Worms (Wo, Sugaki, 1955): as the name implies, curved and irregular cpy exsolution bodies in the shape of worms (Figures 2.3, 2.7), grading into equant blebs in places[4] (Figures 2,4, 2.7). The distinction between equant Wo and P types is largely genetic, and may not always be obvious morphologically.

Emulsion (Em, Ramdohr, 1969): minute and rounded cpy bodies, usually occupying the center of matrix grains, and not exceeding 2-3 μm in diameter (Figure 2.8).

Coarsened W bodies (i.e., lenticular W-forms) are not considered separately, since their shape, though influenced by growth and coarsening, remains basically similar to that of the early W bodies.

The most common natural textures involving bn-cpy intergrowths and ascribed to exsolution, belong to the mutual boundary and W types (Edwards, 1954; Ramdohr, 1969). Some examples of the former are shown in Figures 2.9 and 2.10. Natural W textures have been described, for example, by Van der Veen (1925, Figure 46), and Ramdohr (1969, Figures 180a, 180b, 355, and 356). The textures of Figures 1.1 (page 4) and Figure 2.11 show scattered, coarsened linear bodies

---

[4]This type may grade into the "mutual boundary" type, resulting when the minerals involved show "smooth, regularly curved contacts, without very decided projections of one mineral into the other" (Edwards, 1954).

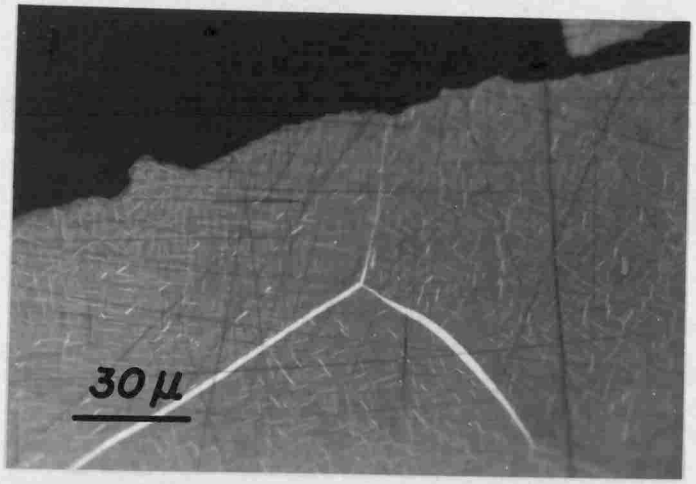

Figure 2.2. Cell and Widmanstätten texture; 12% cpy charge annealed 3 weeks at 150° C (gray: bn; white: cpy).

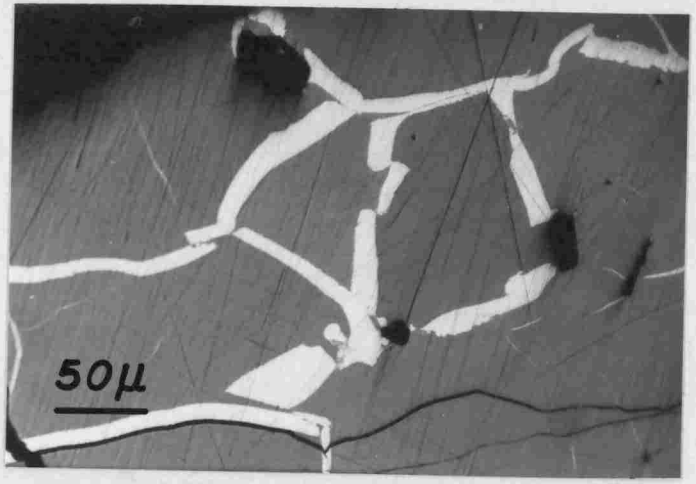

Figure 2.3. Cell texture breaking down and coarsening; 12% cpy charge annealed 4 days at 250° C (gray: bn; white: cpy).

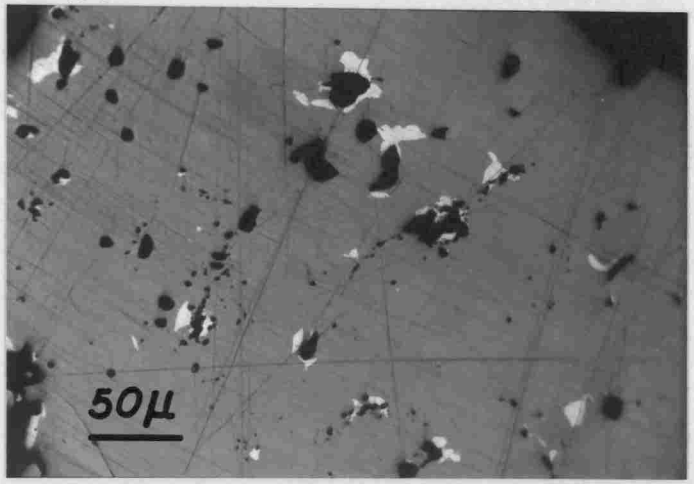

Figure 2.4. Coarsened patches around holes; 25% cpy charge annealed 6 hours at 250° C (gray: bn; white: cpy).

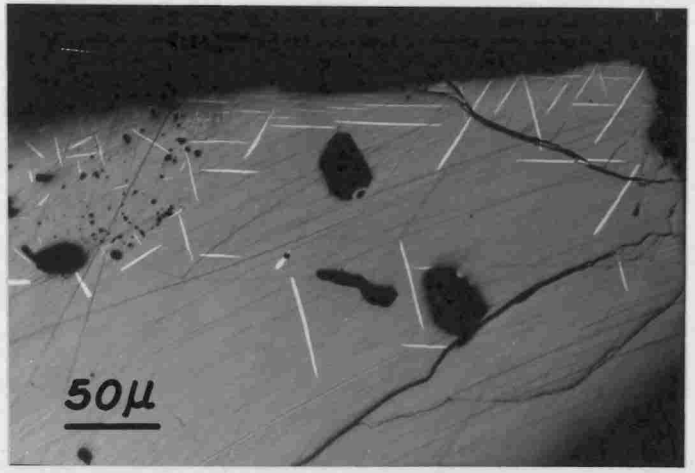

Figure 2.5. Large Widmanstätten lamellae; 25% cpy charge annealed 1 day at 150° C (gray: bn; white: cpy).

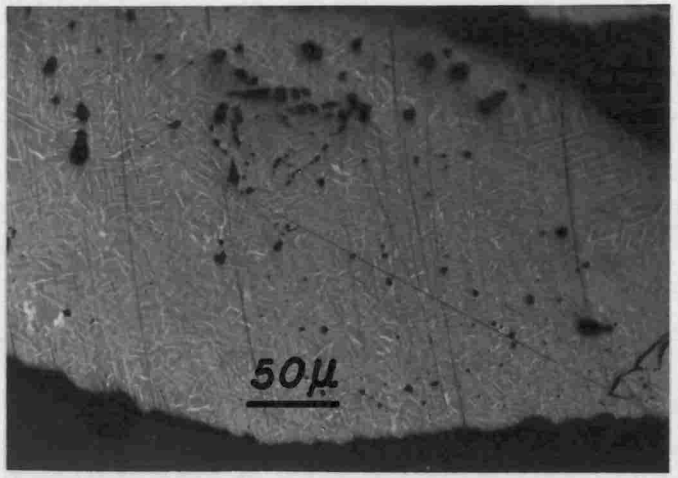

Figure 2.6. Pervasive Widmanstätten texture; 25% cpy charge annealed 10 weeks at 100° C (gray: bn; white: cpy).

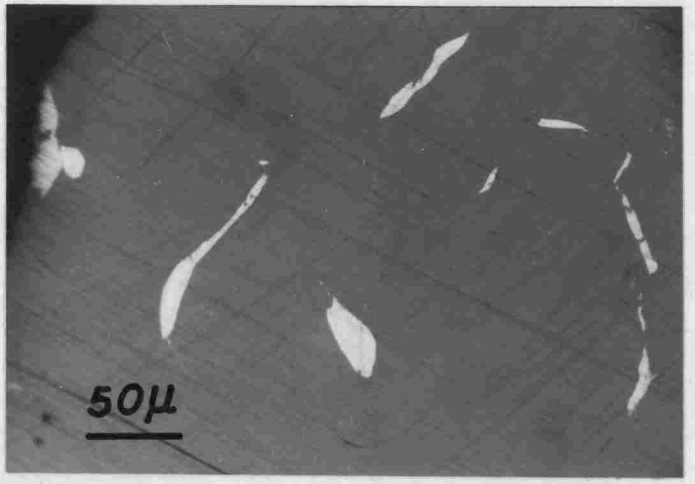

Figure 2.7. Worms due to breakdown and coarsening of a cell texture; 12% cpy charge annealed 4 days at 250° C (gray: bn; white: cpy).

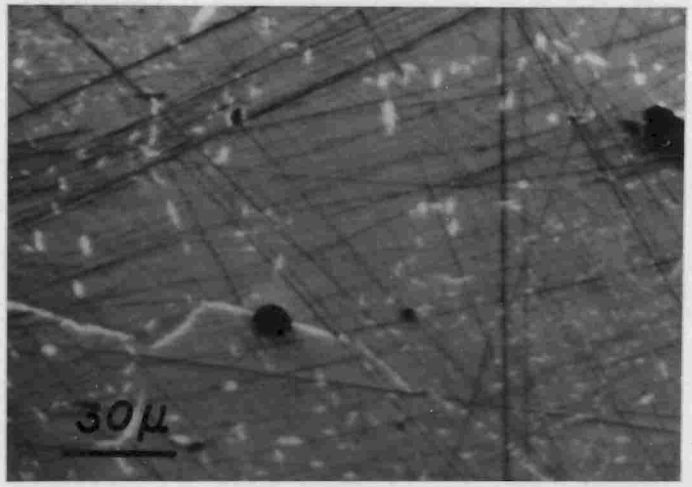

Figure 2.8. Minute Widmanstätten lamellae coarsening into emulsion bodies (gray: bn; white: cpy).

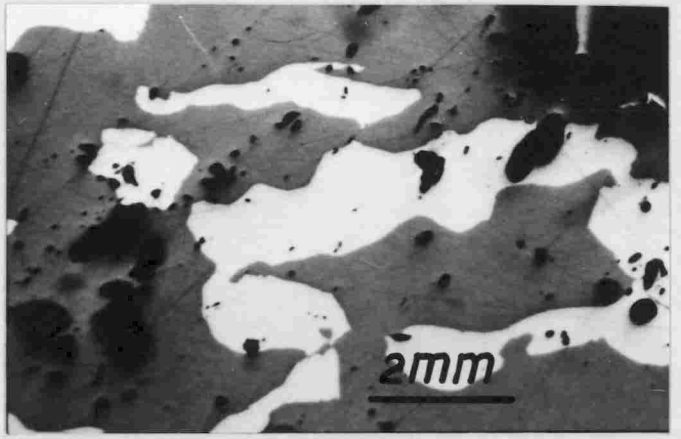

Figure 2.9. Mutual boundary texture; Butte, Mont. (gray: bn; white: cpy).

Figure 2.10. Sample showing a mutual boundary texture; Butte, Mont. (gray: bn; white: cpy).

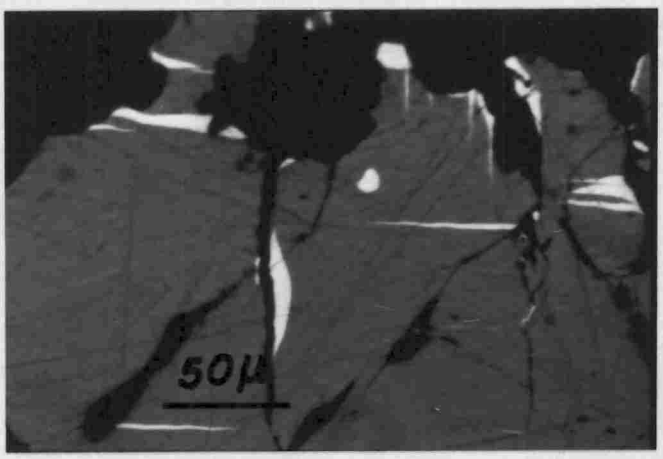

Figure 2.11. Mutual boundary and lamellar texture; Chino, New Mex. (gray: bn; white: cpy).

departing from, or developed along cracks or grain boundaries, and do not seem to reflect true W textures. Figures 1.1 (page 4) and 2.10 were taken from different spots on the same polished section.

Textural Development Model

The previous section was concerned with a purely geometric description of the textural types obtained experimentally. In this section, an attempt is made to note systematic variations of single textural forms as a function of the main parameters involved in the experiments, i.e., composition, annealing temperature, and annealing time. Such variations were fit into a three-dimensional model, the topology of which is shown schematically in the block diagram of Figure 2.12. Isopleth, isochronous, and isothermal diagrams were constructed in order to define the model, but only the first two types of representation are shown (Figures 2.13-2.15 and 2.16-2.18, respectively). The former is effective in depicting how textural evolution proceeds with time at different temperatures, and is similar in principle to the time-temperature-transformation (T-T-T) diagrams used in metallurgy to describe phase transformations. The latter is somewhat similar to a TX phase diagram (Figure 2.1, page 8) and allows an estimate of the degree of supersaturation for each experimental charge.

The experimental points (Appendix A, Table A.1), are represented by dots. Parentheses enclosing the textural symbols introduced previously indicate that the corresponding forms occur in minor amounts. Textural changes from one form to another with time are referred to as "steps." The textural fields shown in the graphs define

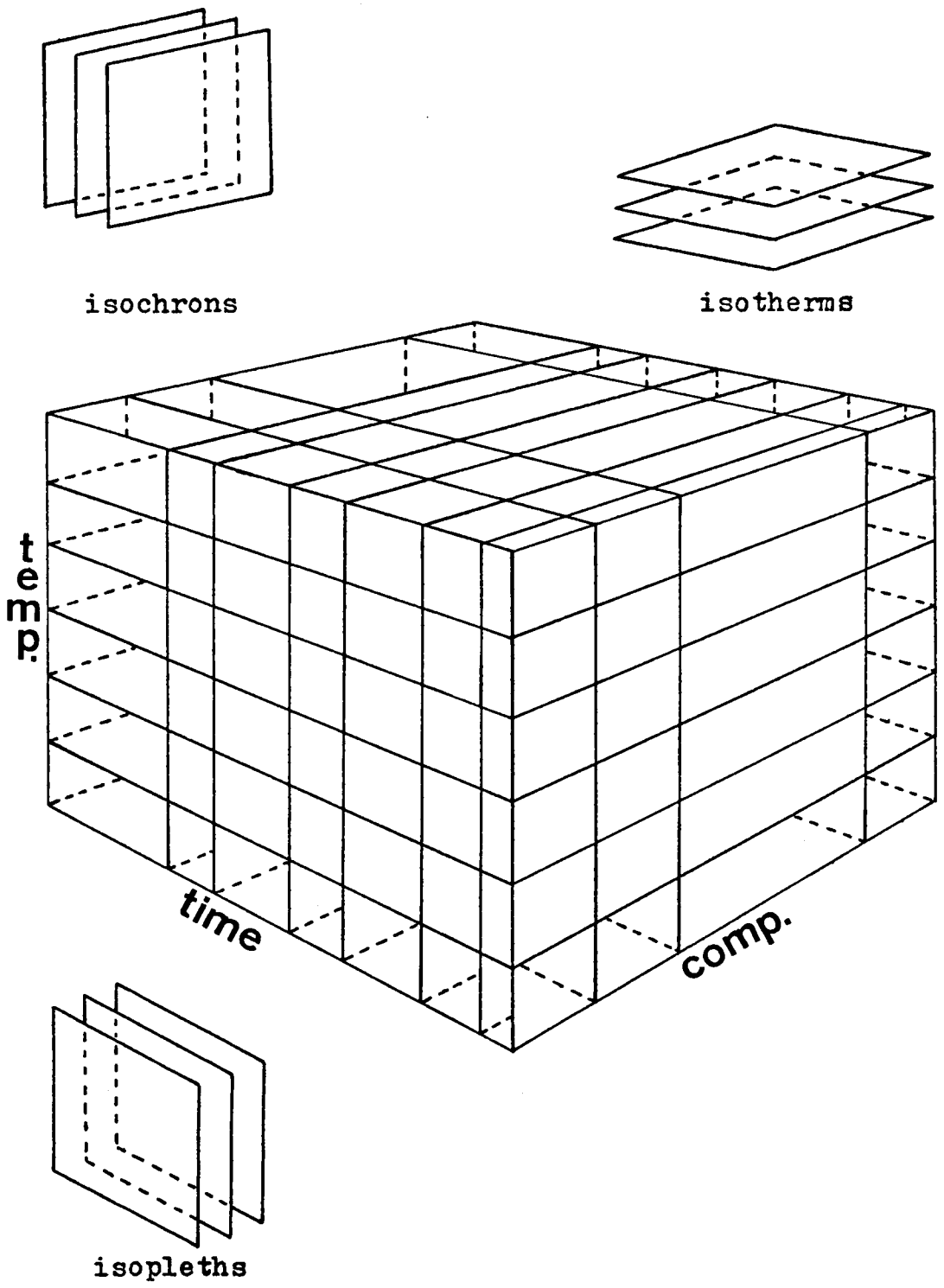

Figure 2.12. Block diagram showing the reciprocal relations of isopleth, isochronous, and isothermal sections.

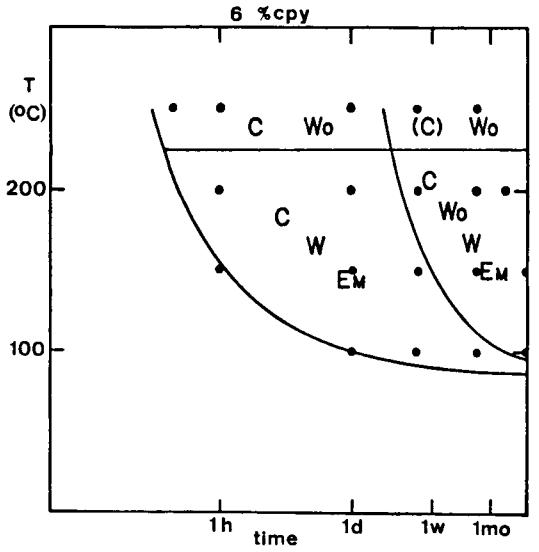

Figure 2.13. T-T-T (isopleth) diagram showing textural evolution in the bn-cpy system; 6% cpy charges. Dots; experimental points. Symbols are explained in the text.

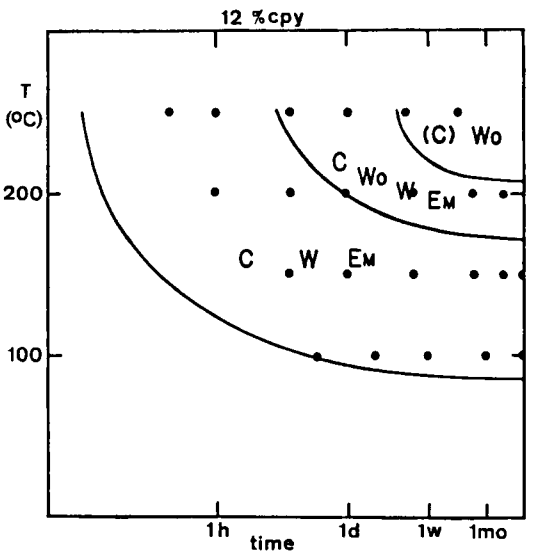

Figure 2.14. T-T-T (isopleth) diagram showing textural evolution in the bn-cpy system; 12% cpy charges. Dots: experimental points. Symbols are explained in the text.

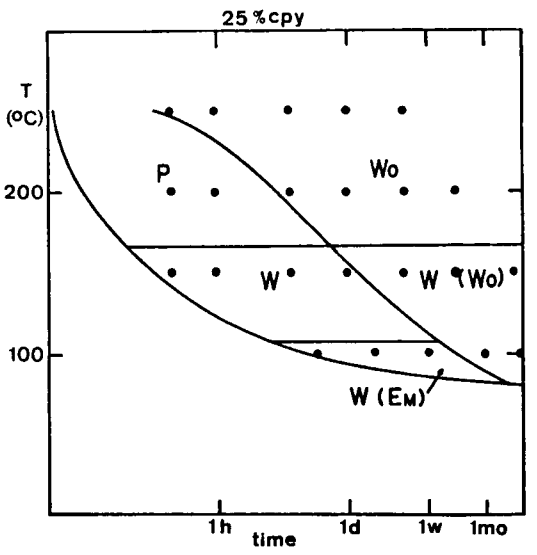

Figure 2.15. T-T-T (isopleth) diagram showing textural evolution in the bn-cpy system; 25% cpy charges. Dots: experimental points. Symbols are explained in the text.

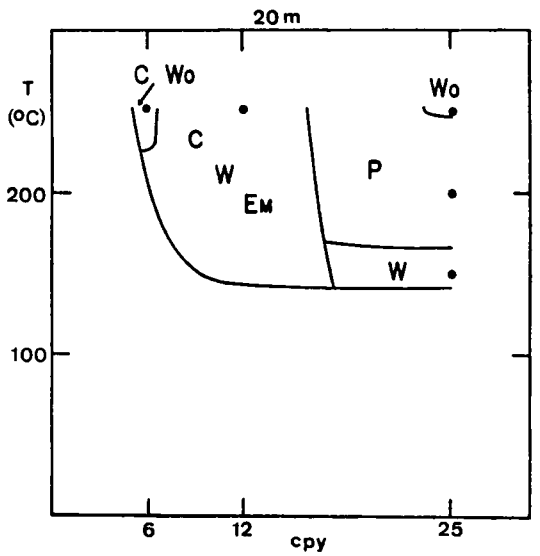

Figure 2.16. Isochronous diagram showing exsolution textures in the bn-cpy system; 20-minute annealing. Dots: experimental points. Symbols are explained in the text.

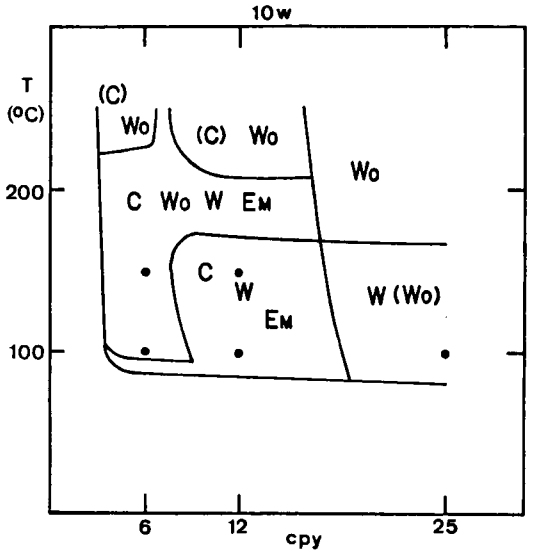

Figure 2.17. Isochronous diagram showing exsolution textures in the bn-cpy system; 10-week annealing. Dots: experimental points. Symbols are explained in the text.

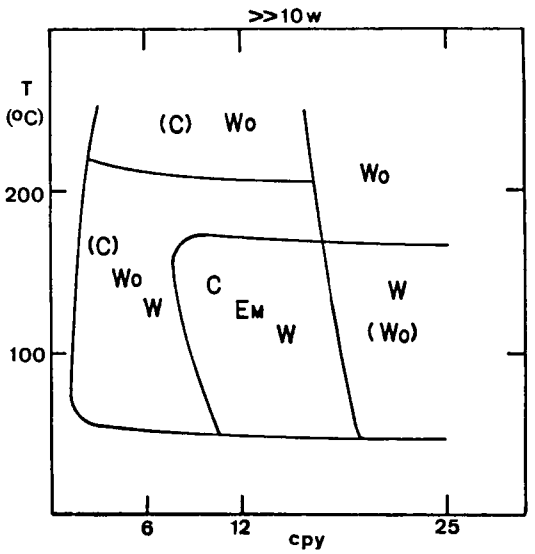

Figure 2.18. Exsolution textures predicted in the bn-cpy system after annealing times much greater than 10 weeks. Symbols are explained in the text.

associations of single forms ("textural assemblages"). In most cases, textural assemblages were determined by microscopic observation. However, they were inferred in those regions for which no experiments are available. No attempt was made to distinguish "inferred" from more or less "definite" boundary curves (for instance by using dotted lines in the former case and continuous lines in the latter), since considerable uncertainty is always present concerning their position. Textural examination revealed the following:

1. C-forms are observed under a wide variety of experimental conditions, but are virtually absent at high degrees of supersaturation (25% cpy, Figure 2.15). At lower degrees of supersaturation (i.e., 6 and 12% cpy, Figures 2.13 and 2.14), they are among the earliest forms observed at all temperatures. However, their relative importance decreases with time, because the early cpy segregations surrounding the bn grains do not grow uniformly throughout their length, but become thicker in places. Subsequent coarsening and spheroidization may produce partial breakdown of the cell structure (Figure 2.3, page 16). The resulting cpy segments may become worm-shaped, reflecting the step C → Wo, but in some cases appear as blebs (Figure 2.7, page 17).

2. P-forms are best developed at the highest degree of supersaturation (25% cpy) and relatively high temperatures (250° and 200° C), where they represent the dominant textural type (Figures 2.4 and 2.15, pages 16 and 21). In all other cases, P-forms are subordinate to absent.

3. W-forms are abundant in all charges at 150° and 100° C over the entire duration of the experiments (up to 10 weeks). The same holds

true for charges with 6 and 12% cpy at 200° C (Figures 2.13 and 2.14). However, no W-forms are observed in 25% cpy charges at 200° C (Figure 2.15). At 250° C, W lamellae are only present in 12% charges annealed for less than 6 hours (Figure 2.14).

4. Wo-forms develop in more than one way. For example, at the lower degrees of supersaturation (i.e., in 6 and 12% cpy charges, Figures 2.13 and 2.14), they form through the breakdown of C-forms and, less commonly, through growth of Em-forms. In charges with a higher degree of supersaturation (i.e., 25% cpy, Figure 2.15), however, they are due to growth and coarsening of P-forms at 250° and 200° C, and partial spheroidization of large W lamellae at the lower temperatures.

5. Em-forms are common in 6 and 12% cpy charges annealed at 200°, 150°, and 100° C up to 10 weeks (Figures 2.13 and 2.14), because they derive from the spheroidization of small W lamellae, which are present under these experimental conditions.

At this point, it is important to note that the development of W lamellae with time is greatly influenced by their original size. W lamellae from charges with 6 and 12% cpy are relatively small (with a maximum width of 1 μm and a length/width ratio normally not exceeding 10 at all temperatures). Usually, they are also close to each other (Figure 2.2, page 16). W lamellae in 25% cpy charges annealed at 150° C, on the other hand, are substantially larger. For example, they measure up to 5 μm in width, with a length/width ratio between 10 and 20 after 2 weeks, and are scattered in the matrix (Figure 2.5, page 16). Charges with 25% cpy, annealed at 100° C (Figure 2.6, page 17), produce pervasive

W-forms with relatively large dimensions (i.e., with a maximum width of about 2 μm, and a length/width ratio of 10-20).

When small W lamellae undergo growth and coarsening, their shape is often altered following the step W → Em (Figure 2.8, page 17). This prevents the development of larger lamellae resulting, instead, in the establishment of Em and, possibly, of equant Wo. In 6 and 12% cpy charges annealed at 200°, 150°, and 100° C, however, small lamellae are observed even after several weeks along with Em-forms, suggesting late exsolution not followed by significant growth and/or coarsening (Figures 2.13 and 2.14, page 21).

The shape of the larger lamellae is not greatly affected with time, since growth and coarsening produce larger, lenticular bodies. However, some scattered lamellae may assume Wo morphologies following the step W → Wo, and rarely develop into blebs.

A schematic representation of the most common steps involved in textural development in the bn-cpy system is given in Figure 2.19.

Effect of Trace Elements

It was shown (Yund and Hall, 1970) that trace amounts of large atoms such as As, Sb, and Bi, which may substitute for S in sulfides, retard the exsolution of pyrite from pyrrhotite. Selenium, also a large atom which substitutes for S in sulfides, is found both in bn and cpy in amounts up to 200 ppm (Sindeeva, 1964). In an attempt to determine whether Se has any effect on cpy exsolution from bn-cpy solid solutions and on bn-cpy textural development, isothermal experiments were performed on 12% cpy charges doped with 500 ppm Se (Appendix A, Table A.1). The ensuing textures did not show any

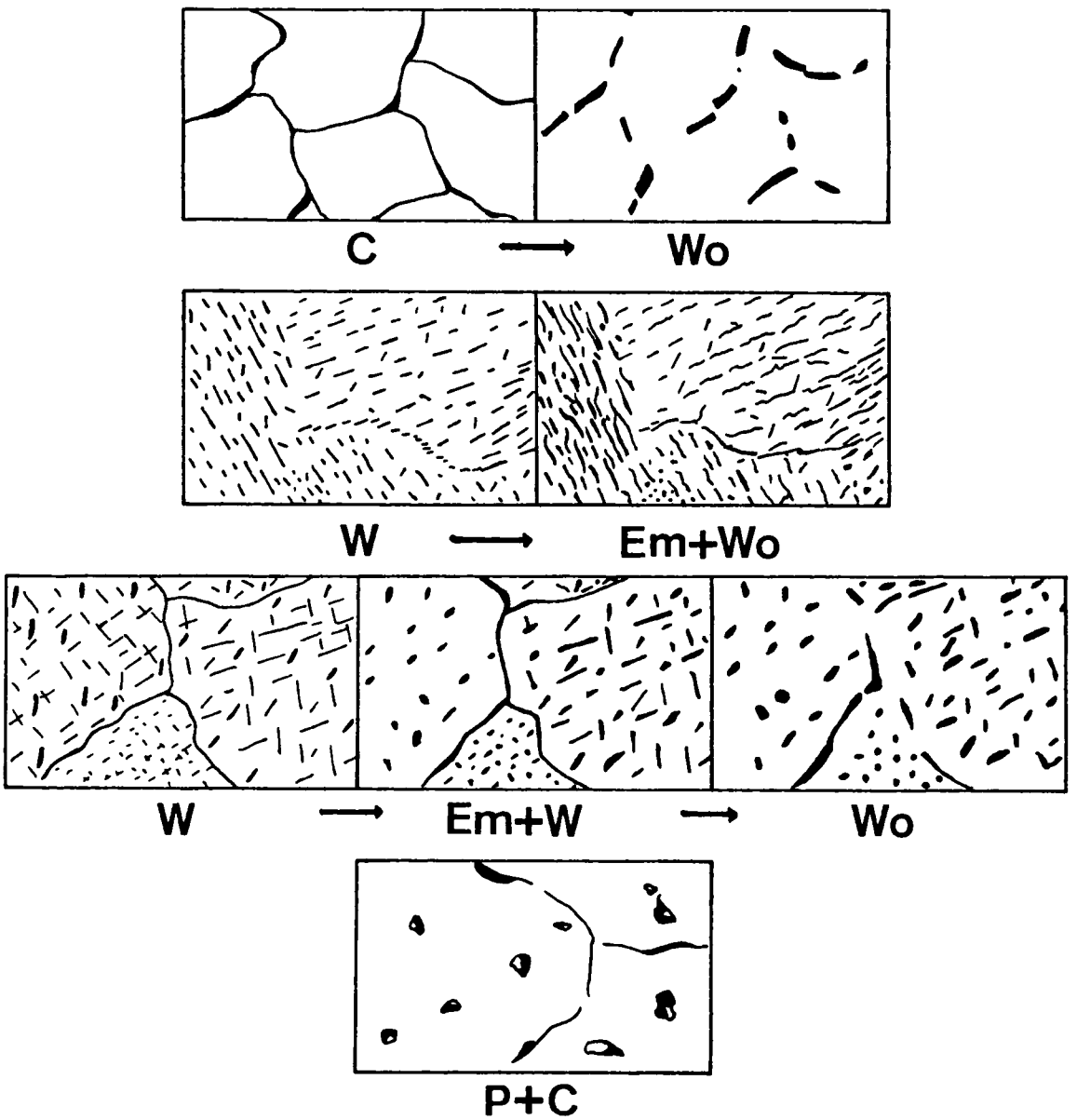

Figure 2.19. Schematic representation of the most common evolutionary steps affecting early textural forms in the bn-cpy system (white: bn; black: cpy). C: cells; P: patches; W: Widmanstätten; Wo: worms; Em: emulsion.

significant differences from those obtained using undoped charges under identical experimental conditions, despite early indications to the contrary, which were based on a limited number of experiments (Durazzo and Taylor, 1978).

Coarsening Experiments

The effect of temperature on the coarsening of large W lamellae was also investigated. Charges containing 30% cpy, which had produced dominant large W-forms on quenching from 800° C, were annealed at 150° C for one week. This temperature was chosen because it had not produced substantial coarsening on large W lamellae in 25% cpy charges, and was deemed adequate to produce larger lamellae by growth. Subsequently, the charges were annealed for 4 weeks at 200°, 250°, 300°, and 350° C (Appendix A, Table A.2).

Coarsening of the existing W lamellae increased with the annealing temperature, as was expected. While the original shape was largely retained at 200° C and only partly retained at 250° and 300° C (Figures 2.20 and 2.21), it almost completely disappeared at 350° C, to yield Wo-forms. At the same time, fresh exsolution occurred at grain boundaries, yielding C-forms which were rare at 200°, common at 250° and 300° C, and mostly coarsened and broken down, yielding Wo-forms, at 350° C. Fresh exsolution also took place throughout the matrix grains at all the temperatures of the experiments, producing a second generation of minute, pervasive W lamellae (Figure 1.2, page 4), which seldom coarsened to form Em bodies. They differed from the lamellae formed on quenching, which were considerably larger in size.

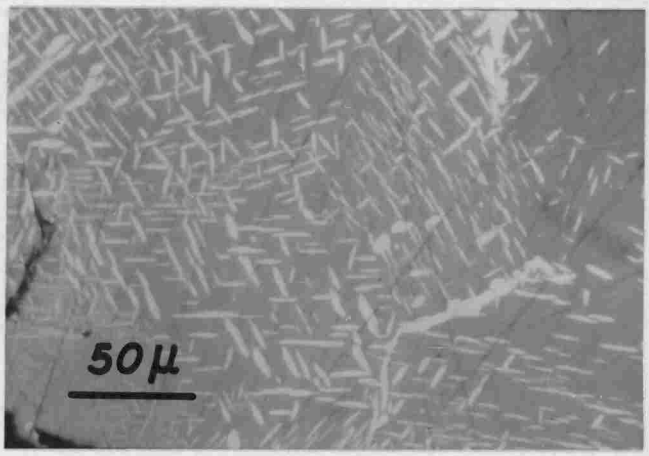

Figure 2.20. Coarsening Widmanstätten lamellae and coarsening cell texture; 30% cpy charge annealed 1 week at 150° C and 4 weeks at 250°C (gray: bn; white: cpy).

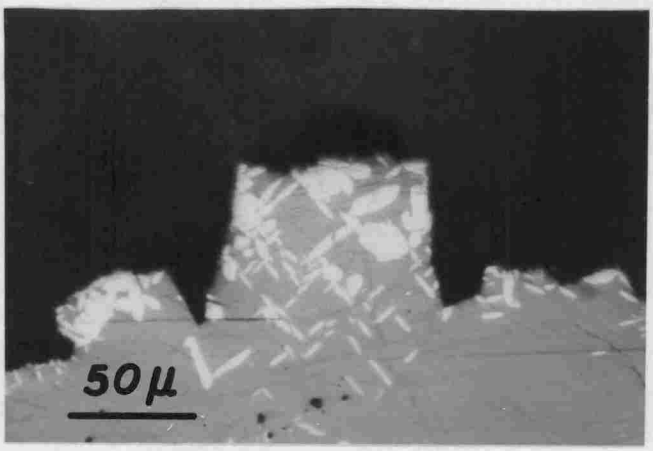

Figure 2.21. Coarsening Widmanstätten lamellae and worms tending to produce a mutual boundary texture in places; 30% cpy charge annealed 1 week at 150° C and 4 weeks at 250° C (gray: bn; white: cpy).

These experiments indicate that no chemical equilibrium was achieved during annealing at 150° C, as would have been desirable. However, despite the effect of growth, which also alters the shape of the lamellae, the experimental results indicate that large W lamellae are erased at about 250° C. The possibility exists that annealing times far in excess of several weeks may lower this temperature substantially.

Interpretation of the Experimental Textures

In the following discussion an attempt is made to explain textural evolution in the bn-cpy system in light of thermodynamic and kinetic considerations commonly applied to metallurgical as well as sulfide systems (e.g., Stanton and Gorman, 1968; Brett, 1964; Yund and Hall, 1970; Birchenall, 1973).

The relationship between textural forms and different values of temperature and composition, expressed in Figures 2.16-2.18 (page 22) for different annealing times, is represented schematically in Figures 2.22 and 2.23. These apply, respectively, to dominant early and mature forms.

Early forms. The textures shown in Figure 2.22 are consistent with the view that the types of nucleation and growth involved in the establishment of early textural features are associated with given levels of the energy responsible for exsolution, and are influenced by the prevailing values of the diffusivities. It should be pointed out, in this connection, that the chemical free energy difference involved in the early stages of exsolution—commonly referred to as "driving

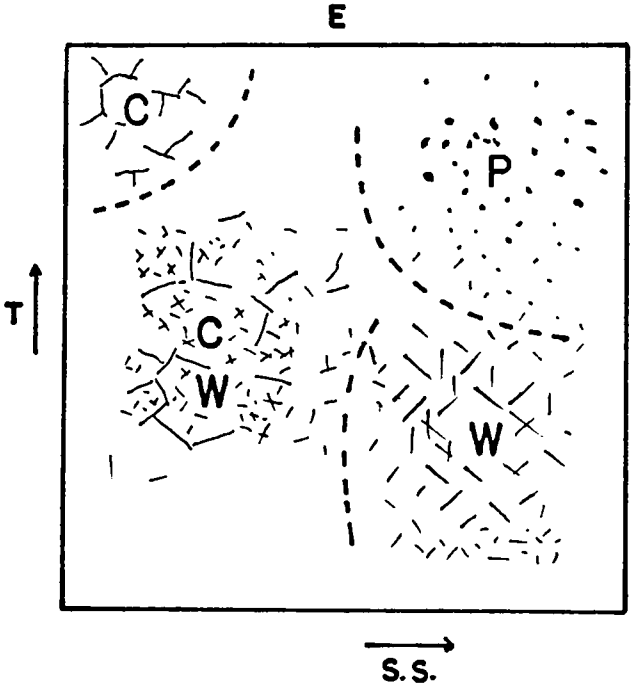

Figure 2.22. Schematic representation of early (E) exsolution textures in the bn-cpy system. T: temperature; S.S.: degree of supersaturation.

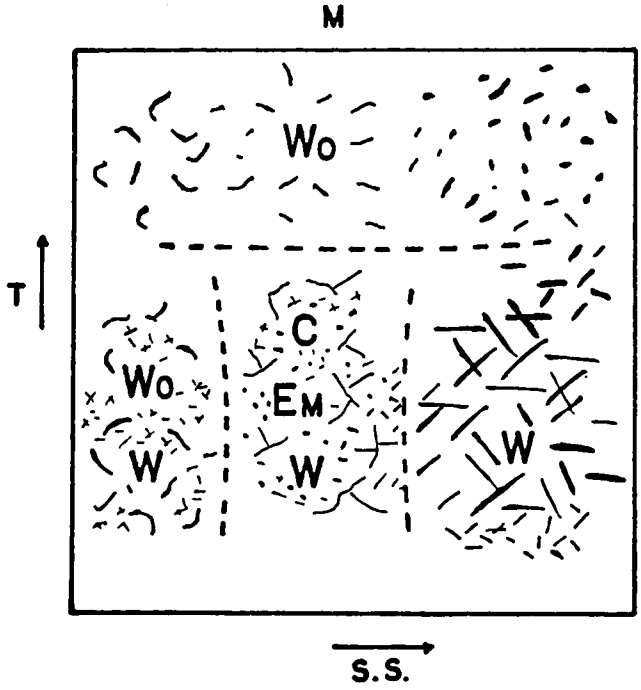

Figure 2.23. Schematic representation of mature (M) exsolution textures in the bn-cpy system. T: temperature; S.S.: degree of supersaturation.

force"—is directly related to the initial degree of supersaturation (see, for instance, the excellent review of Yund and McCallister, 1970, on exsolution). It is also important to remember that the formation of nuclei introduces a surface (or interface) free energy term and, normally, a strain-free energy term, both of which oppose nucleation. The barrier against nucleation due to these opposing factors is greater within the matrix grains than at grain boundaries because, in the latter case, while new surface bounding the nucleus is created, old surface separating the matrix grains is destroyed. The result is removal of the energy stored at grain boundaries (see, for instance, Shewmon, 1969).[5] This is consistent with the observation that in the bn-cpy system C-forms, typically associated with relatively low degrees of supersaturation (i.e., 6 and 12% cpy charges), develop along cracks and grain boundaries at all temperatures. W-forms, observed inside the matrix grains, may require a greater driving force to develop than C-forms, even if both forms coexist at intermediate degrees of supersaturation (12% cpy, Figures 2.16 (page 22) and 2.22). The distribution of W-forms, and their coarsened products (i.e., Em), in relation to the initial degree of supersaturation is compatible with such an interpretation (Figures 2.22 and 2.23).

Charges with the highest degree of supersaturation (25% cpy) annealed at 250° and 200° C, however, produce dominant P-forms rather

---

[5] In addition, Clemm and Fisher (1955) calculated that the energy barrier to nucleation is lower at grain corners (4-grain junctions) than at grain edges (3-grain junctions), and lower at grain edges than at grain boundaries (2-grain junctions). This relationship was further discussed by Cahn (1956).

than W-forms. An explanation for the presence of P-forms and lack of W-forms must take into account the diffusion patterns relevant to the system under study.

Cations normally diffuse many orders of magnitude faster than S in sulfides (e.g., Condit et al., 1974); thus, the major role in cpy exsolution from bn solid solution is played by Cu and Fe. Barton and Skinner (1967) pointed out that the reaction kinetics involving Cu sulfides are generally more rapid than those involving Fe sulfides, while reaction rates relevant to Cu-Fe sulfides are intermediate between those of Cu and Fe sulfides. This would indicate that the mobility of Cu in sulfides is greater than that of Fe.

However, Chen and Harvey (1975) obtained activation energies for the self-diffusion coefficients of Fe and Cu in cpy of 6.4 kcal/mole and 12.1 kcal/mole, respectively, between 100° and 300° C. These results indicate that over this temperature range, the diffusivity of Fe in cpy considerably exceeds that of Cu, because diffusivities vary exponentially in relation to the activation energies in diffusion processes. Samal and Gilevich (1978) measured Cu self-diffusion in $Cu_{4.9}Fe_{1.1}S_4$ and $Cu_{1.1}Fe_{1.1}S_2$ at 600° C, obtaining nearly identical values in both cases. Assuming a similar behavior at lower temperatures, it may be inferred that Fe diffuses faster than Cu in bn, as it does in cpy, at the temperatures of the present experiments. In addition, three times as many Cu atoms must leave cpy nucleation sites as Fe atoms must reach them, for cpy exsolution from bn to proceed. Thus, Cu diffusion appears to control nucleation and growth in the bn-cpy system.

It is possible that at high degrees of supersaturation (i.e., 25% cpy), the diffusivity of Cu increases relatively to that of Fe, generating much higher growth rates than at lower degrees of supersaturation. Under these conditions, growth might become dominant over nucleation. The result would be the establishment of fewer and larger precipitates.[6]

In the case in point, the P-forms could be the expression of nucleation at 3- or 4-grain junctions. These sites are favored over others on energetic grounds (Clemm and Fisher, 1955). Thus they would experience the earliest possible nucleation events at 250° and 200° C, where the degrees of supersaturation (and the undercooling) are less pronounced than at lower temperatures. At 150° and 100° C, on the other hand, a greater driving force might promote nucleation and growth mostly along crystallographic directions within the grains—producing large and sparse W patterns—and only marginally at grain boundaries.

Evidence was sought that P-forms originate at 3- or 4-grain junctions in the 250° and 200° C charges. According to Schneiderhöhn (1952), etching with a concentrated solution of I-KI can best disclose the grain structure of a bn polycrystalline aggregate. However, this procedure only revealed pseudo-structures consisting of a network of cracks bearing no relation to the grain boundaries. Structural etching,

---

[6]Growth rates are a direct function of diffusivities (e.g., Yund and McCallister, 1970). While temperature strongly controls diffusivities according to the Arrhenius equation $D = D_0 \exp(-Q/RT)$ (D = diffusivity; D_0 = constant; Q = activation energy; R = gas constant; T = temperature in °K), the composition of a solid solution may also have an important bearing on diffusivities (Kurtz et al., 1955; Birchenall, 1973), and thus affect growth rates.

as Ramdohr (1969) warns, is very difficult to obtain in bn, even using the proper etchants.

Mature forms. The previous discussion applies to early forms, which develop mainly through nucleation and growth when the matrix still maintains a substantial amount of the initial supersaturation, and are not greatly affected by such processes as grain coarsening and spheroidization. In the establishment of mature forms, on the other hand, the latter processes, along with growth, are perhaps the most important, while nucleation assumes a secondary role (e.g., Verhoeven, 1975).

Figures 2.22 and 2.23 show that the mature forms are, in general, conditioned in their development by the early types from which they evolve. For instance, Wo-forms are found where either C or P were the early forms. However, the evolution of early textural patterns may not always be predictable. This is the case in assemblages consisting of several forms, all equally well developed. In such a situation, evolutionary steps expected to affect a given form may not take place because of competition from the other forms present. Thus, in 12% cpy charges annealed at 100° C, C-forms do not evolve into Wo-forms to a significant extent, but are largely retained, while some of the early W-forms coarsen to yield Em-forms (Figures 2.18 (page 22) and 2.23).

Widmanstätten textures. The small, pervasive W-forms obtained during the present experiments on coarsening seem identical in shape and size, to the small forms obtained in the isothermal experiments (Figures 2.2, 2.13, and 2.14 (pages 16 and 21). Probably, they

are also similar to the W-forms which Brett (1964) ascribed to secondary exsolution in a depleted matrix. They normally coexist with C- and Em-forms (e.g., in most 6 and 12% cpy charges). As the matrix becomes less supersaturated, following early exsolution, further nucleation takes place in those available sites for which the barrier against nucleation is least effective. If these sites coincide with given crystallographic directions, it is likely that the precipitates will be coherent with the matrix, as long as their size does not exceed certain values, after which coherency may be lost (e.g., Martin and Doherty, 1976).

Late nucleation throughout a depleted matrix is compatible with limited growth and the retention of a large number of minute, coherent or semicoherent lamellae. A configuration of this type may entail some degree of deformation at the matrix-precipitate interface. This, in turn, implies relatively high strain energy. However, the preservation of structural continuity across the matrix-precipitate interfaces minimizes the tension due to the surface energy term, thus conferring a certain stability to the system (textural stability is discussed in standard textbooks of physical metallurgy, e.g., Verhoeven, 1975; Martin and Doherty, 1976).

The above discussion suggests an explanation for the existence of two kinds of W patterns in the present experiments which, however, involved annealing times not exceeding 10 weeks. The small, pervasive lamellae are the likely outcome of nucleation and growth in a matrix with a very low degree of supersaturation, which allows some amount of coherency to be maintained at the matrix-precipitate interface. The

large lamellae, which often assume a lenticular shape, are probably produced by rapid growth affecting few nucleation sites in a highly supersaturated matrix. Under these conditions, coherency may be lost as the size of the precipitates increases, but no substantial spheroidization takes place below about 250° C due to the large size involved. The loss of coherency entails a decrease in strain energy and an increase in surface energy (e.g., Verhoeven, 1975). The latter, however, does not make a substantial positive contribution to the total free energy of the system, because of the relatively small interface area associated with the large precipitates.

Comments on the Textural Development Model

Some observations concerning the experimental results and their representation in the diagrams of the previous section (i.e., Figures 2.13-2.18 (pages 21-22) are in order. First, the boundary curves are not as well defined as shown. Their position is purely indicative, since the relative abundance of the textural types present within each field varies in a gradual and continuous fashion. This is not surprising, because textural evolution is governed largely by interface and strain energy changes, which are substantially lower than the chemical free energy changes responsible for phase transformations. For example, the total free energy change for exsolution in a typical metal alloy system may be 2 to 3 orders of magnitude greater than the surface and strain energy terms associated with precipitates measuring about 1-5 μm across, and making up about 25% of the total volume (Martin and Doherty, 1976).

Secondly, during textural development, it is common to observe the appearance of new textural forms at the expense of preexisting ones. These appearances, however, do not necessarily entail the disappearance of the preexisting types. For example, not all C-forms may evolve into Wo-forms; some can be retained to yield a textural assemblage of the type C+Wo, or (C)+Wo, if the C-forms become subordinate.

Thirdly, the presence of only one phase below about 50° C after times far greater than 10 weeks (Figure 2.18, page 22) is speculative. It may be justified by the occurrence in nature of nonstoichiometric bornites, to be discussed in the next section, but does not imply that such an occurrence reflects thermodynamic equilibrium conditions. On the contrary, it may reflect metastability.

Finally, although the textural development model is based on isothermal experiments, it has considerable geologic relevance, since it indicates under which conditions given textural features develop. Knowledge of the relationship between textural forms and the parameters involved in their formation helps in predicting textural development during slow cooling or heating due to metamorphism, assuming different initial conditions of temperature, composition, and preexisting textural configurations.

Limitations inherent in this approach concern the maximum time of the experiments, which is short in a geologic context. As a result, the experiments may fail to reveal which textures are present after long geologic times. However, the isothermal results are applicable in principle to predicting textural development relevant to cooling or heating. By analogy, the T-T-T diagrams describing phase transformations as well as textural changes in metallurgical systems, which are

constructed by isothermal experiments, show almost identical trends as similar diagrams based on cooling experiments. The boundary curves in the latter, however, are shifted to slightly lower temperatures and longer times.

As an example of how textural development can be predicted on the basis of isothermal experiments, it is difficult to expect abundant W textures during slow cooling along the bn-cpy join, since prolonged exposure to temperatures above 250° C would produce mutual boundary textures (Figures 2.18 and 2.23, pages 22 and 30). Small W-forms could possibly originate, in minor amounts, below 200° C (Figure 2.1, page 8), but might also be erased by coarsening during the geologically-significant times associated with cooling slightly below 200° C. Mutual boundary textures such as are observed at Butte (Figure 2.10, page 18) do not show W-forms; on the other hand, most natural W lamellae are fairly wide (i.e., 3 μm) and have length/width ratios greater than 10 (Van der Veen, 1925; Ramdohr, 1969).

E. GEOLOGIC IMPLICATIONS

The development of mutual boundary textures in bn-cpy intergrowths is possible when the diffusivities of the atoms involved—and therefore the prevailing temperatures—are high enough as to allow pronounced coarsening and spheroidization. The experimental results of this study indicate that such conditions are met at temperatures in excess of about 250° C after several weeks, and probably at lower temperatures after substantially longer annealing times. Therefore, bn-cpy mutual boundary textures can get established through exsolution

by slow cooling from temperatures above the solvus (Figure 2.1, page 8). However, they can also develop when simultaneous precipitation of bn and cpy takes place.[7] Examples of mutual boundary textures in Cu mineral deposits are given in Figures 2.9 and 2.10 (pages 17 and 18).

The presence of dominant lamellar forms is more difficult to interpret. Extremely rapid cooling from temperatures above the solvus, which produces dominant W textures (Schwartz, 1931a), appears unlikely except, possibly, in cases involving small mineralized bodies.[8]

Exsolution from an extremely diluted matrix during slow cooling could possibly account for the establishment of W patterns below about 200° C, where a polymorphic transformation from cubic to orthorombic bn solid solution occurs (Brett, 1963; Koto and Morimoto, 1975). Some of the cooling experiments performed by Brett at 3° C/day (1964) suggest such a possibility, since they produced W patterns along with non-lamellar forms. However, the former were subordinate. In addition, the maximum cooling time of Brett's 1964 experiments (183 days from 600° to 50° C) is only indicative in relation to the cooling times involved in geologic processes.

---

[7] No attempt is made in the present discussion to analyze the possibility of co-precipitation from aqueous solution and its textural implications. For the sake of completeness, however, it is pointed out that such a possibility may exist.

[8] Throttling, as discussed by Barton and Toulmin (1961), though capable of explaining rapid cooling in theory, may not apply to many actual cases, and should in each instance be compatible with field evidence.

Long exposure to high temperatures below the solvus (Figure 2.1, page 8) would result in continuous re-equilibration and extremely low degrees of supersaturation. These conditions promote nucleation and growth at grain boundaries. In addition, coarsening and spheroidization of small cpy lamellae—likely to exsolve inside bn solid solution grains—would occur to a much greater extent than is possible during the short times of controlled experiments, probably even at 200° C and slightly lower temperatures.

There are instances, however, of well-developed bn-cpy W intergrowths in mineral deposits. The size of the cpy lamellae in bn is relatively large, varying between 3-5 μm wide and 25-150 μm long (Lauterberg, Germany, Van der Veen, 1925, Figure 46; Ramdohr, 1969, Figures 180b and 356; the Ida mine, Namibia, Ramdohr, 1969, Figure 180a; and Svappavaara, Sweden, Ramdohr, 1969, Figure 355). The prevalence of wide and continuous W lamellae in a bn matrix rules out slow cooling from high temperatures for the ores of these locations.

Two possible alternatives to explain include replacement and exsolution due to heating of a supersaturated bn solid solution formed metastably at room temperature.

The first alternative is suggested by the work of Ray (1930), who obtained W-like cpy lamellae by exposing bn to distilled water under pressure at 80°-100° C, and Schouten (1934), who produced W cpy patterns similar to exsolution textures by reacting bn with a concentrated solution of $3FeSO_4 \cdot Fe_2(SO_4)_3$ at 85° C. Although morphologic criteria exist in theory to distinguish W textures due to exsolution from similar textures due to replacement (Newhouse, 1928; Schwartz,

1931b), both experimental work and observation of natural ores have questioned their reliability (Schouten, 1934; Edwards, 1954; Ramdohr, 1969). Therefore, replacement is not to be ruled out in light of present knowledge.

The second possibility is suggested by the experimental results of this study. It was noted during the preceding discussion on W textures that charges with a high degree of supersaturation (25% cpy) annealed at 150° and 100° C produce dominant lamellar forms characterized by relatively large dimensions (Figures 2.15 and 2.22, pages 21 and 30). However, slow cooling rules out the possibility that high degrees of supersaturation will be maintained to temperatures at which large lamellae can develop and be retained. On the other hand, heating of supersaturated bn solid solutions could produce high enough values for the diffusivities, so as to trigger exsolution throughout the matrix, in a fashion compatible with the initial degree of supersaturation. The lamellar forms produced by this process could be retained, provided the maximum temperature achieved did not exceed a value at which pronounced coarsening and spheroidization can occur—i.e., about 250° C or, perhaps, a few tens of degrees lower.

Examples of metastable bornites which exsolve cpy lamellae on heating (also called "anomalous," "sulfur-rich," or "x" bornites) are known in nature (Wandke, 1926; Morimoto et al., 1960; Prouvost, 1960; von Gehlen, 1963; Brett and Yund, 1964; Sillitoe and Clark, 1969). It has been suggested that their origin could be primary, i.e., due to precipitation from mineralizing fluids (Yund and Kullerud, 1966), or secondary, i.e., due to supergene processes affecting preexisting

bornite or other copper minerals (Frenzel, 1959; Brett and Yund, 1964; Tufar, 1967; Sillitoe and Clark, 1969).

Anomalous bornites deviating substantially from stoichiometric Cu_5FeS_4 were produced experimentally by reacting synthetic bn with acidified ferric sulfate solutions below 35° C (Dutrizac et al., 1970). Such a reaction is geologically possible, as oxydation of ubiquitous pyrite producing H_2SO_4, $FeSO_4$, and $Fe_2(SO_4)_3$ is a common occurrence in nature.

F. CONCLUSIONS

The isothermal experiments described in this study add considerably to the understanding of the bn-cpy intergrowths found in nature. The following points emerge:

1. Mutual boundary textures result from coarsening and spheroidization above about 250° C or, possibly, slightly lower temperatures. Accordingly, they are compatible with:
    a. Simultaneous formation of bn and cpy at temperatures above 500° C;
    b. Exsolution during slow cooling from above the solvus;
    c. Metamorphism to temperatures above about 250° C.
2. It is difficult to explain Widmanstätten textures as due to exsolution during slow cooling from temperatures above the solvus because, under these conditions, continuous re-equilibrium would occur, producing mostly exsolution along bn grain boundaries. In addition, Widmanstätten lamellae, which can originate in a dilute matrix below 200° C, might be erased during the extremely long annealing times

prevailing during slow cooling, even below 200° C. Two processes may explain Widmanstätten textures in nature:

a. Replacement; and

b. Exsolution from anomalous bornites during heating to low temperatures (i.e., not exceeding values lying between 200° and 250° C). The existence of anomalous bornites in nature is well documented, and their genesis is consistent with both experimental and field evidence.

CHAPTER III

THE KINETICS OF EXSOLUTION INVOLVING MSS-PENTLANDITE AND THEIR BEARING ON THE INTERPRETATION OF NATURAL PYRRHOTITE-PENTLANDITE TEXTURES

A. INTRODUCTION

It was pointed out in the general introduction that, despite repeated efforts by many researchers, textural features in sulfide mineral assemblages have, in most cases, not been fully explained. Barton (1970) emphasized both the difficulties and potential rewards involved in textural studies, noting that "the interpretation of ore textures is the most maligned, most difficult, and most important aspect" of the study of sulfide rocks.

The present investigation was aimed at interpreting some of the textural features observed in the mineral deposits loosely called "Sudbury-type ores." These consist dominantly of Fe, Ni, and Cu sulfides, and are mined in several areas of Canada, the Soviet Union, Australia, and southern Africa. For some time, they have represented the most important source of nickel in the world.

Most deposits in the Sudbury district contain varying amounts of chalcopyrite, pyrite, cubanite, and magnetite, as well as other sulfides and oxides, in addition to the basic pyrrhotite (po = $Fe_{1-x}S$)-pentlandite (pn = $(Fe,Ni)_9S_8$) assemblage (Hawley, 1962).

From a textural standpoint, the most peculiar characteristic associated with nickel sulfide ores are probably those concerning the

mutual relationship of po and pn (e.g., Hawley and Haw, 1957; Hawley, 1962; Kullerud, 1963b; Naldrett et al., 1967; Misra and Fleet, 1973). These studies indicate that natural po-pn intergrowths are the result of exsolution during cooling from temperatures compatible with a magmatic origin (i.e., > 900° C if the mafic to ultramafic origin of the associated silicate rocks is taken into account). Therefore, it was felt that an investigation concerning the exsolution kinetics relevant to this mineral pair could contribute significantly to a better understanding of the history of nickel sulfide deposits. The stabilities and phase relations of these minerals are fairly well known from phase equilibria studies within the Fe-Ni-S system. This proved to be of significant importance and made the present study feasible. Preliminary results of this investigation were given by Durazzo and Taylor (1977).

B. PREVIOUS STUDIES

Countless descriptions of Ni-sulfide deposits exist in the literature. These include, for example, the comprehensive description of the Sudbury district by Hawley (1962), and other detailed studies of individual deposits, such as those of Strathcona (Naldrett and Kullerud, 1967); Marbridge, Québec (Graterol and Naldrett, 1971); Yilgarn, western Australia (Barrett et al., 1977).

Phase equilibria studies involving the Fe-Ni-S system are particularly relevant to this investigation, since they have provided a great deal of information concerning the possible mechanism of Ni-sulfide ore formation and textural development. Lundqvist (1947), Kullerud (1956, 1963a), Craig et al. (1967b), Craig and Kullerud (1969),

and Kullerud et al. (1969) defined the system as a whole. That part of the system relevant to the formation of po and pn, and to their stabilities, was studied in detail by several investigators. Kullerud (1963b) determined the upper stability of pn and the processes by which it may form. Naldrett et al. (1967) defined the monosulfide solid solution (mss)[1] phase boundaries between 600° and 300° C. Shewman and Clark (1970) defined the phase boundaries of pn between 600° and 400° C. Misra and Fleet (1973) investigated the phase boundaries of pn between pn between 600° and 230° C, and compared the composition of synthetic pentlandites with that of a number of natural pentlandites from Canadian mines. Craig (1973) studied the mss-pn phase relations between 300° and 150° C.

Hawley and Haw (1957) produced synthetic mss-pn textures by cooling synthetic mss of varying compositions in a N_2 stream from 800° C. They obtained pn blebs, lenses, and flames oriented in one direction in the mss matrix, and massive segregations along mss grain boundaries. Some among the resulting intergrowths closely resembled those of natural ores. Solid solutions with a high Ni content yielded "peculiar Widmanstätten intergrowths," consisting of pn developed in "narrow blades along three intersecting directions" in the mss matrix, along with the types described previously. In all the experiments, S was allowed to escape during cooling. Therefore, the influence the bulk composition (in particular the S content) may have on textures could not be assessed. Consequently, the experimental results by Hawley and Haw

---

[1]The mss field includes pyrrhotite and millerite, stretching from the Fe-S to the Ni-S join at temperatures above 992° C (Kullerud et al., 1969).

(1957) though indicative, do not fully reveal which factors control textural development in Ni-sulfide deposits.

Crystallographic studies dealing with the orientation relationship between po host and exsolved pn are important in connection with po-pn textural interpretation. Francis et al. (1976) determined by x-ray precession studies that po and pn form oriented intergrowths, and defined their mutual relations.

C. EXPERIMENTAL PROCEDURE

Mss members (Table 3.1 and Figure 3.1)[2] were synthesized in sealed, evacuated silica-glass tubes from high-purity elements, according to the techniques described by Kullerud (1971). Before synthesis, Fe and Ni sponge (both Johnson Matthey Chemical Ltd., grade 1, 99.998% spec. pure) were reduced in a hydrogen stream at 900° C for over 2 hours, in order to eliminate any trace of oxides. Sulfur (99.999+%) was from ASARCO.

The charges were brought gradually to 800° C and left at that temperature for 3 hours. Subsequently, they were quenched in water, reground in a diamonite mortar under toluene to a particle size of about 0.2 mm, sealed in new tubes under vacuum, and placed in a vertical furnace at 1200° C for 30 minutes. This temperature exceeds the melting

---

[2]Although not many data are available concerning the average bulk composition of Ni sulfides from single mines, Naldrett and Kullerud (1966) estimated the average composition for most such ores to vary between 2-10% Ni and 37-40% S, the balance consisting mostly of Fe.

Table 3.1

Composition of the Experimental Charges
Used in the Present Study

Weight %			Atomic %		
Fe	Ni	S	Fe	Ni	S
57.0	6.0	37.0	44.83	4.49	50.68
56.5	6.0	37.5	44.30	4.48	51.22
49.5	13.0	37.5	38.92	9.72	51.36
43.0	20.0	37.0	34.00	15.04	50.96
42.5	20.0	37.5	33.51	15.00	51.49

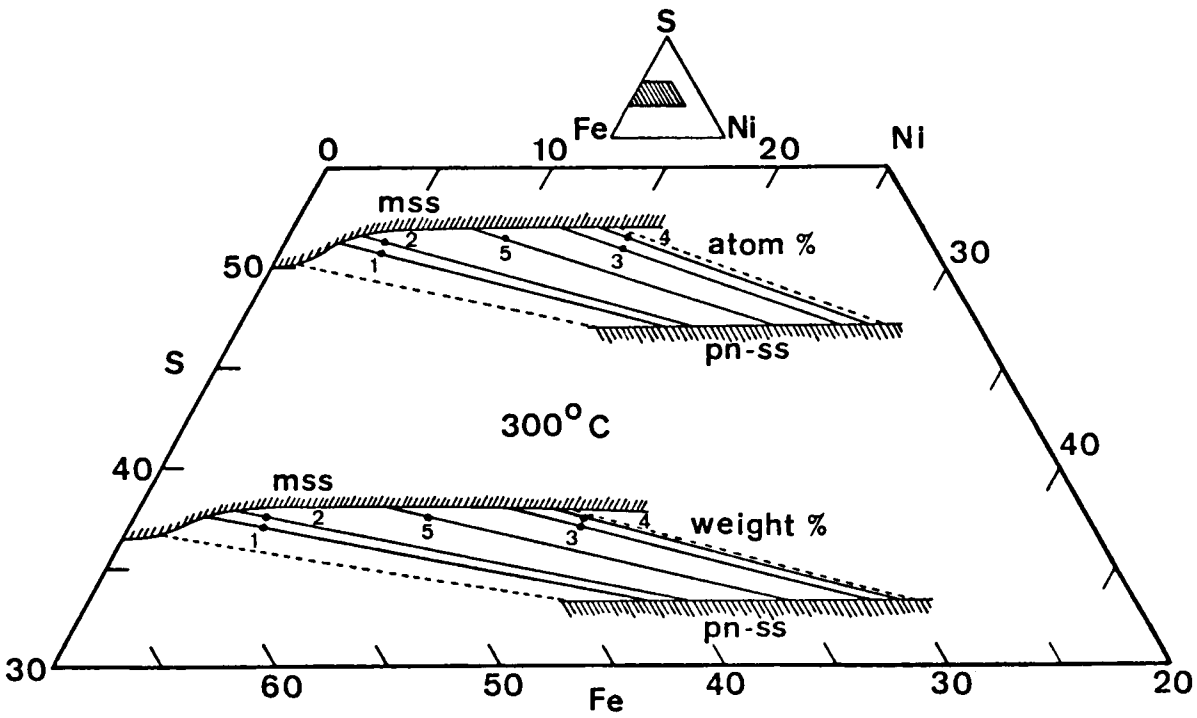

Figure 3.1. Part of the Fe-Ni-S system showing the mss-pn phase relations at 300° C. Points 1-5 represent the compositions used in this study. The stability fields of mss and pn are from Naldrett et al. (1967) and Shewman and Clark (1970) respectively. The dotted tie-lines were determined experimentally by Misra and Fleet (1973). The continuous tie-lines are based on the dotted tie-lines.

temperature of mss of any composition[3] (Kullerud et al., 1969). Following quenching in water, the charges were annealed for a week at 900° C, in order to promote grain growth. Microscopic observation established that the size of the individual grains within each aggregate particle was not uniform, ranging from about 30 μm to 1 mm.

Homogeneity and composition of mss were checked by optical examination in reflected light, electron microprobe analysis, and x-ray diffraction, Individual charges weighing about 20 mg were subsequently annealed at temperatures between 200° and 400° C for times ranging between 20 minutes and 5 weeks, and quenched in cold water. Some charges were used in slow cooling experiments between 500° and 100° C, and quenched in cold water at various temperatures (Appendix B). All charges were examined optically. In some cases, electron microprobe analyses were performed using a fully-automated MAC 400 S instrument, operating at 15 kV, with a beam current of 0.03 μA, spot diameter of 1-2 μm. Synthetic troilite, millerite, and mss were used as standards. Corrections for matrix effects were applied according to procedures described by Ziebold and Ogilvie (1963).

D. PRESENTATION OF RESULTS AND DISCUSSION

Textural Terminology

As in the previous chapter, the textural forms obtained experimentally were conveniently grouped into "early types" and "mature

---

[3]This procedure (i.e., melting the charge) was adopted by Misra and Fleet (1973) in order to obtain a homogeneous product. However, these workers used a blow torch to heat the silica tubes.

types." The two terms indicate, respectively, forms showing limited growth and coarsening, and forms that underwent significant growth and coarsening. The terminology is borrowed from the literature (e.g., Van der Veen, 1925; Edwards, 1954; Ramdohr, 1969) and redefined, in order to avoid confusion.

The early types, whose symbols consist of one letter, include:

Cell (C, Hawley, 1962) or "network" (Van der Veen, 1925): continuous or discontinuous pn veinlets along grain boundaries or cracks in the mss matrix (Figure 3.2). Their maximum width is about 5 μm.

Patches (P): equant pn bodies around holes, cracks, or grain boundaries in the mss matrix (Figure 3.3). Their maximum diameter is 15 μm.

Blades (B): elongated and narrow pn bodies developed along one direction within the mss matrix, often departing from holes, cracks, or grain boundaries (Figure 3.4), but also isolated inside matrix grains. Their maximum width is 1 μm.

Widmanstätten (W, Schwartz, 1931b); or "lattice" (Van der Veen, 1925); "crystallographic" (Schwartz, 1931b); "lamellar" (Ramdohr, 1969): elongated pn lamellae developed along three or more directions, similar to the kamacite/taenite intergrowths described in iron meteorites (Figures 3.5 and 3.6). Normally, the maximum width of the lamellae is about 10 μm. As was done in the previous chapter, coarsened W bodies are not included among the "mature types" described next, since their shape remains basically unaltered despite growth and coarsening.

The mature types, designated by two-letter symbols, include:

Coarsened linear bodies (Cl): This general term includes pn bodies developed along one direction within the mss matrix. They

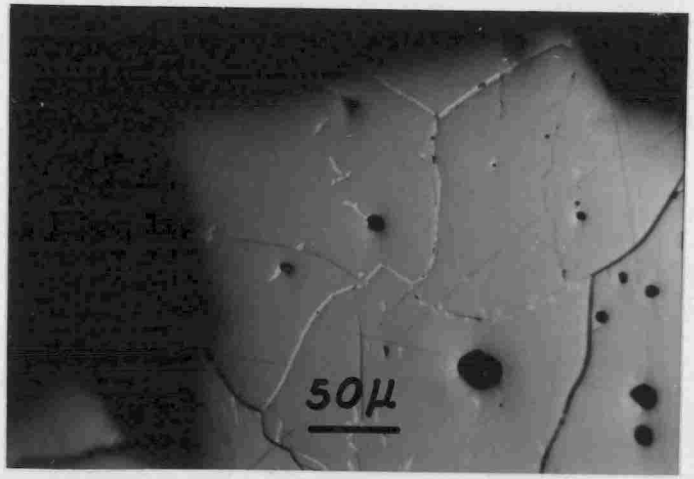

Figure 3.2. Cell texture; 13% Ni; 37.5% S charge annealed 1 hour at 300° C (gray: mss; white: pn).

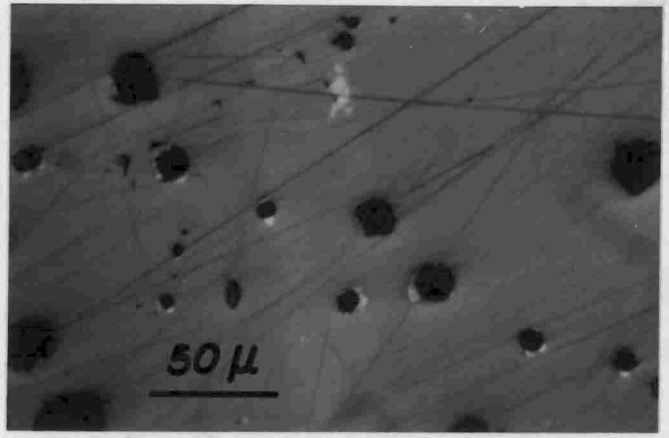

Figure 3.3. Coarsened patches around holes; 6% Ni; 37.0% S charge annealed 6 hours at 400° C (gray: mss; white: pn).

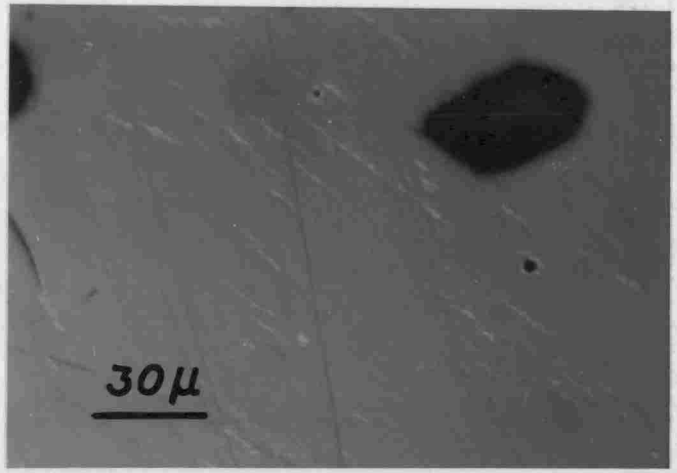

Figure 3.4. Partially coarsened, en échelon blades; 6% Ni, 37.0% S charge annealed 20 minutes at 300° C (gray: mss; white: pn).

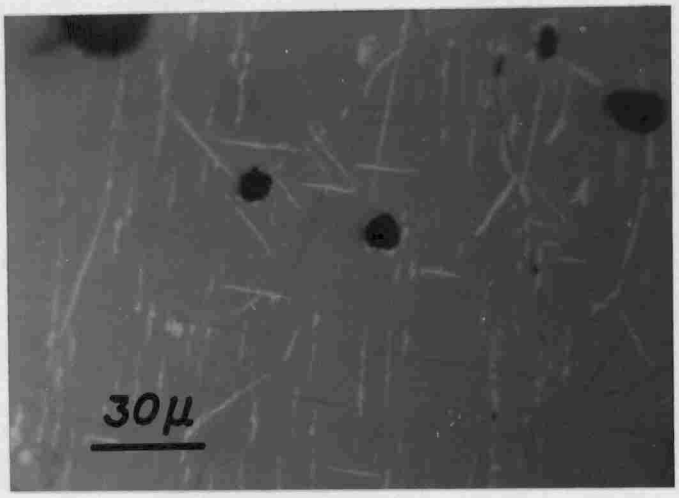

Figure 3.5. Coarsened blades and Widmanstätten lamellae; 6% Ni, 37.0% S charge annealed 1 hour at 300° C (gray: mss; white: pn).

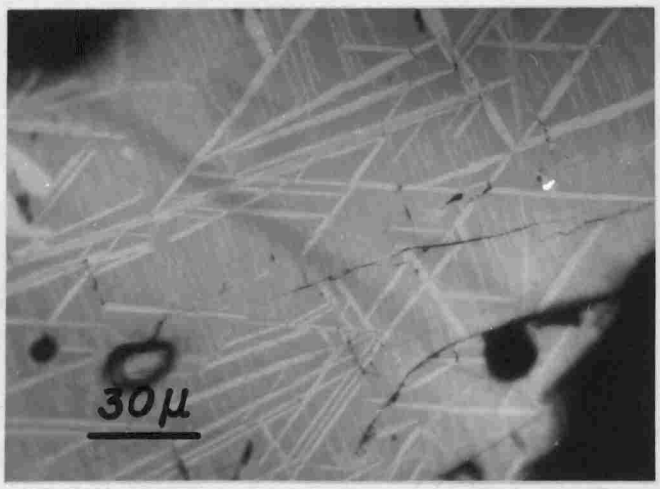

Figure 3.6. Widmanstätten and continuous, pervasive, wirey texture; 20% Ni, 37.0% S charge annealed 5 weeks at 200° C (gray: mss; white: pn).

include wedges (Figures 3.7 and 3.8), wavy lamellae (Figure 3.9), thin narrow, wire-like bodies (Figures 3.6 and 3.10), and aggregates of linear forms similar to the pn flames common in Ni-sulfide ores [Figures 3.11 and 1.4 (page 4)].

Worms (Wo, Sugaki, 1955): curved and irregular pn bodies in the shape of worms (Figures 3.9 and 3.12), often in the form of equant blebs (Figure 3.13). The morphology of equant Wo may be very similar to that of P-forms, though the two types differ genetically.

The textural types found commonly in Ni-sulfide ores are relatively few: e.g., coarsened C, Wo, flames and, less frequently, other forms of the Cl type (e.g., Van der Veen, 1925; Edwards, 1954). In particular, Hawley (1962) recognized three basic types of such intergrowths at Sudbury, as well as in other parts of Canada and in Southern Africa:

1. pn inside po grains, which in some cases produces the characteristic flames [Figures 1.3 (page 4) and 3.14];

2. pn along po grain boundaries, also called "interstitial" pn (Figure 3.14); and

3. large pn ovoids in po, also referred to as "coarse" pn.

Such forms as W and very thin, wirey Cl-forms have not been reported in the geologic literature, while Cl-forms of the type illustrated in Figure 3.9 are not uncommon.

Textural Development Model

In this section, variations in the textural characteristics of the isothermal runs are related to the experimental parameters involved (i.e., composition, annealing temperature, and annealing

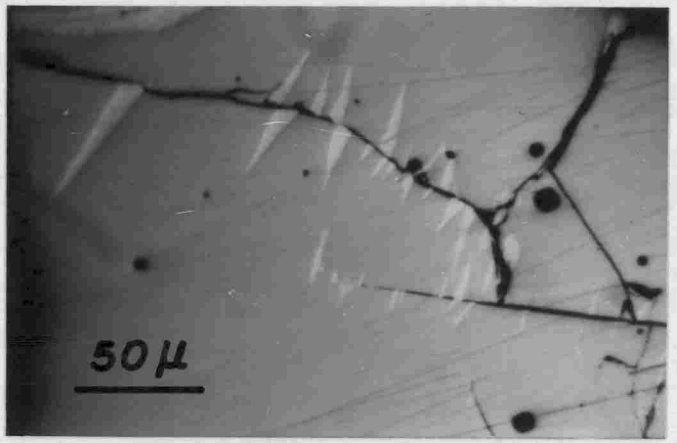

Figure 3.7. Coarsened blades (long wedges); 20% Ni, 37.5% S charge annealed at 300° C (gray: mss; white: pn).

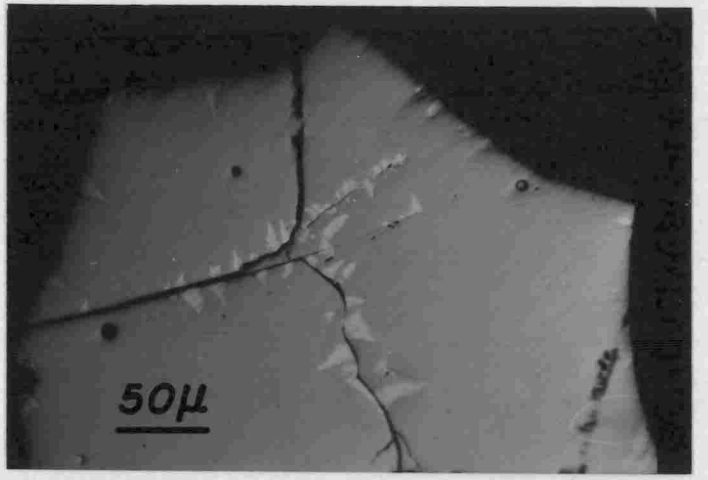

Figure 3.8. Coarsened blades (short wedges); 20% Ni, 37.5% S charge annealed 9 days at 300° C (gray: mss; white: pn).

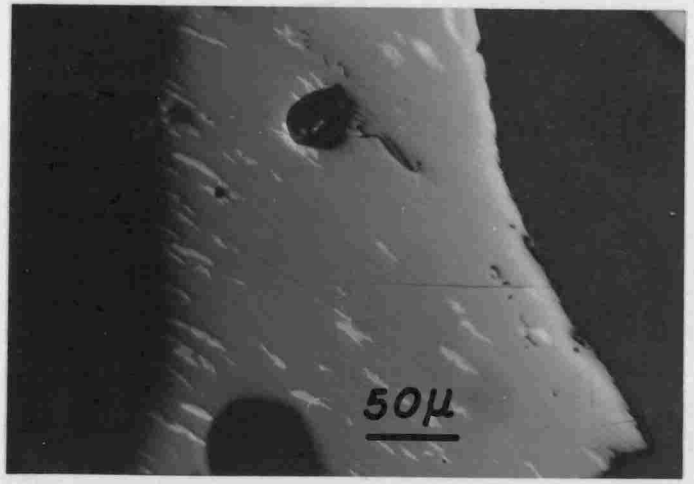

Figure 3.9. Coarsened, en échelon blades; 6% Ni, 37.5% S charge annealed 9 days at 300° C (gray: mss; white: pn).

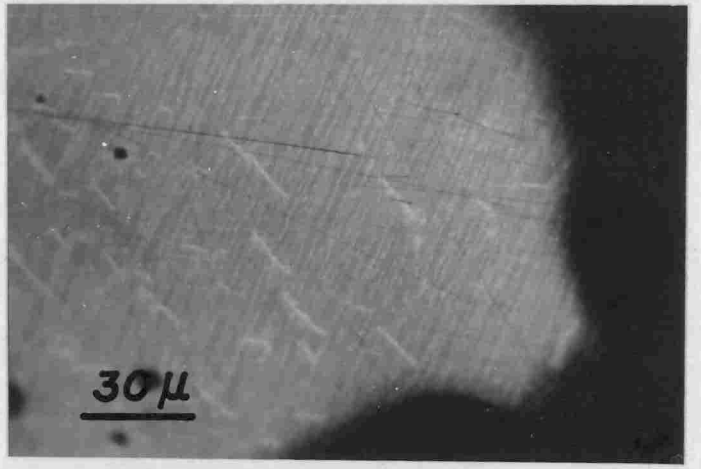

Figure 3.10. Dominant wirey texture; 20% Ni, 37.0% S charge annealed 5 weeks at 200° C (gray: mss; white: pn).

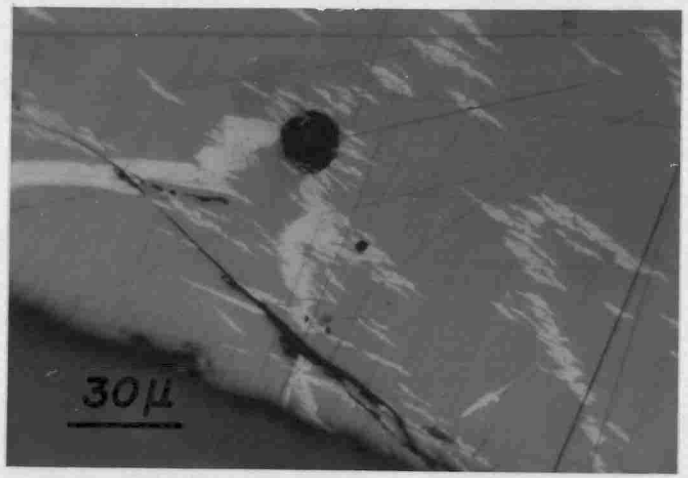

Figure 3.11. Coarsened, en échelon blades with thin terminations, similar to natural flames; 13% Ni, 37.5% S charge annealed 5 weeks at 250° C (gray: mss; white: pn).

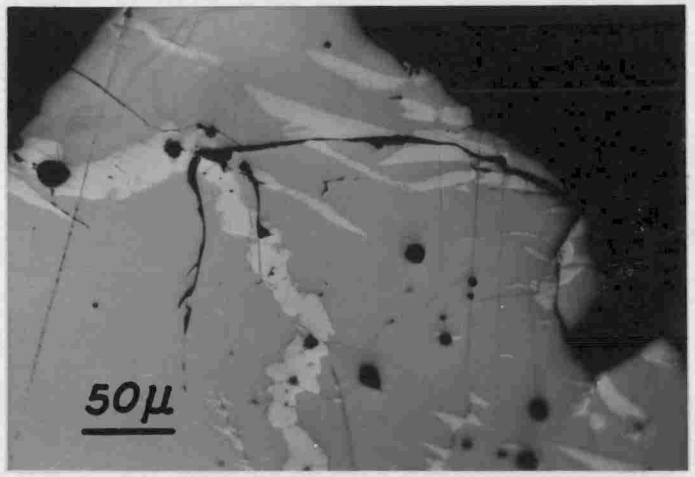

Figure 3.12. Coarsened cell and blades (worms); 20% Ni, 37.5% S charge cooled from 500° to 100° C at 1° C/hour (gray: mss; white: pn).

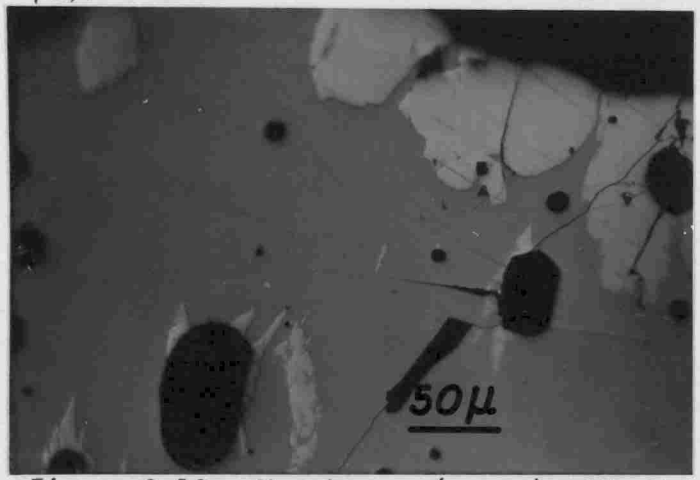

Figure 3.13. Massive pn (worms) with thin, wavy terminations (flames) in places; 20% Ni, 37.0% S charge cooled from 500° to 100° C at 1° C/hour (gray: mss; white: pn).

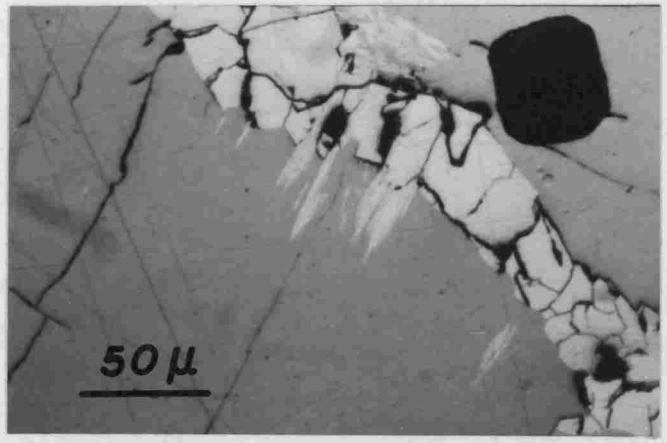

Figure 3.14. Coarsened cell texture and flames; Falconbridge Mine, Sudbury, Ont. (gray: po; white: pn)

time). Following the approach described in Chapter II (Figure 2.12, page 20), three-dimensional models were constructed for each of the joins investigated (6 and 20% Ni). Textural evolution is shown by isopleth and isochronous diagrams (Figures 3.15-3.19 for the 6% Ni join, and Figures 3.20-3.24 for the 20% Ni join). The former type of representation conveniently shows the influence of time and temperature on textures, while the latter provides an estimate for the degree of supersaturation associated with each experimental charge.

It is obvious that along each of the joins considered (i.e., 6 and 20% Ni) the degree of supersaturation decreases with an increase in S content [compare point 1 with 2, and 3 with 4, Figure 3.1 (page 49)]. However, it also appears from Figure 3.1, that in charges with identical S contents, those with the higher Ni content have the higher degree of supersaturation (compare point 1 with 3 and point 2 with 5 and 3).

The experimental points (Appendix B, Table B.1) are represented by dots. Parentheses enclosing the textural symbols introduced previously indicate that the corresponding forms occur in minor amounts. Textural changes from one form to another with time are referred to as "steps." The textural fields shown in the graphs define associations of single forms ("textural assemblages"). In most cases, textural assemblages were determined by microscopic observation. However, they were inferred in those regions for which no experiments are available. No attempt was made to distinguish "inferred" from more or less "definite" boundary curves (for instance by using dotted lines in the former case and continuous lines in the latter), since considerable uncertainty is always present concerning their position. Textural examination revealed the following:

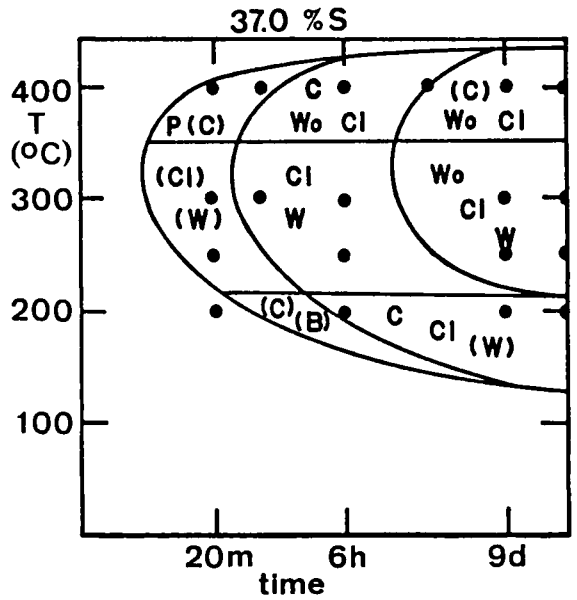

Figure 3.15. T-T-T (isopleth) diagram showing textural evolution in the mss-pn system; 6% Ni join, 37.0% S. Dots: experimental. Symbols are explained in the text.

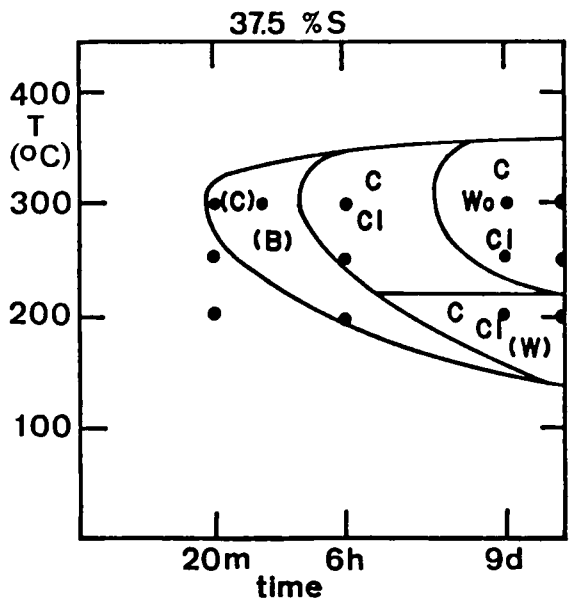

Figure 3.16. T-T-T (isopleth) diagram showing textural evolution in the mss-pn system; 6% Ni join, 37.5% S. Dots: experimental points. Symbols are explained in the text.

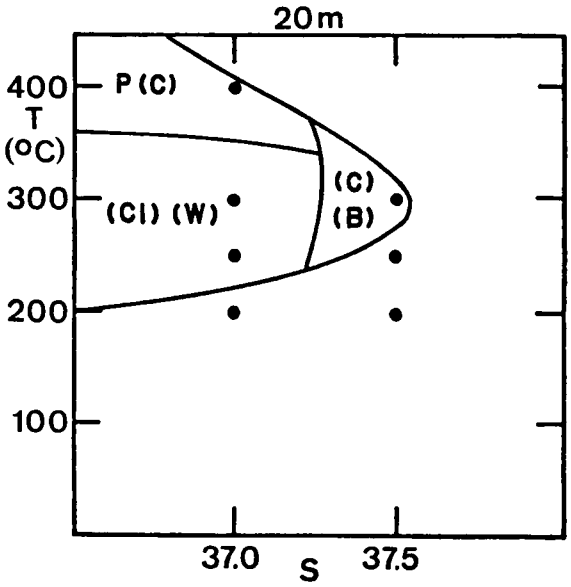

Figure 3.17. Isochronous diagram showing exsolution textures in the mss-pn system; 6% Ni join, 20-minute annealing. Dots: experimental points. Symbols are explained in the text.

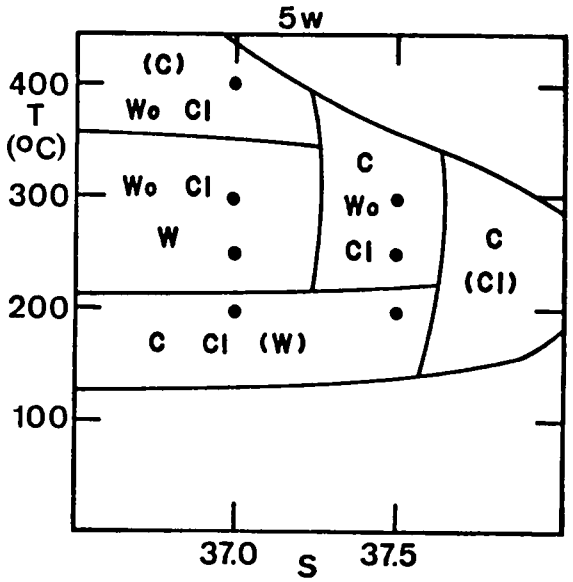

Figure 3.18. Isochronous diagram showing exsolution textures in the mss-pn system; 6% Ni join, 5-week annealing. Dots: experimental points. Symbols are explained in the text.

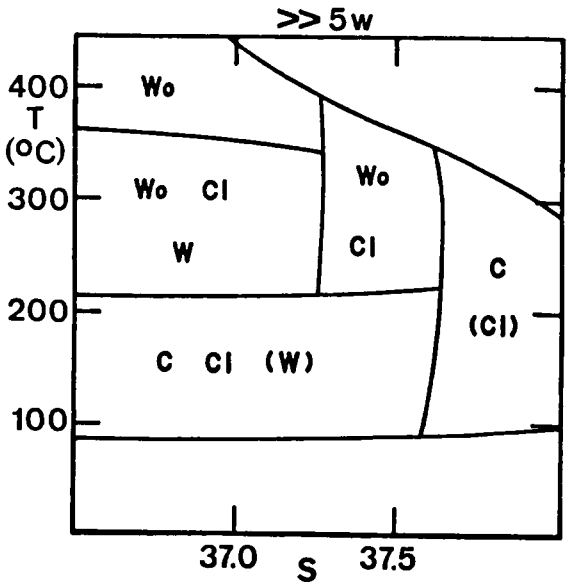

Figure 3.19. Exsolution textures predicted in the mss-pn system, 6% Ni join, after annealing times much greater than 5 weeks. Symbols are explained in the text.

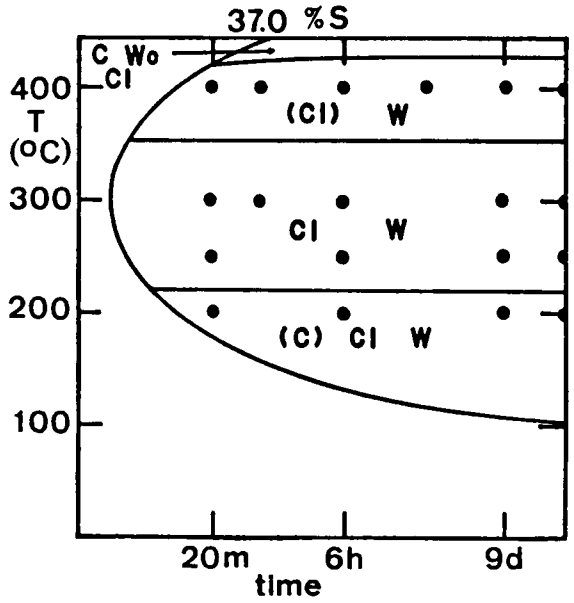

Figure 3.20. T-T-T (isopleth) diagram showing textural evolution in the mss-pn system; 20% Ni join, 37.0% S. Dots: experimental points. Symbols are explained in the text.

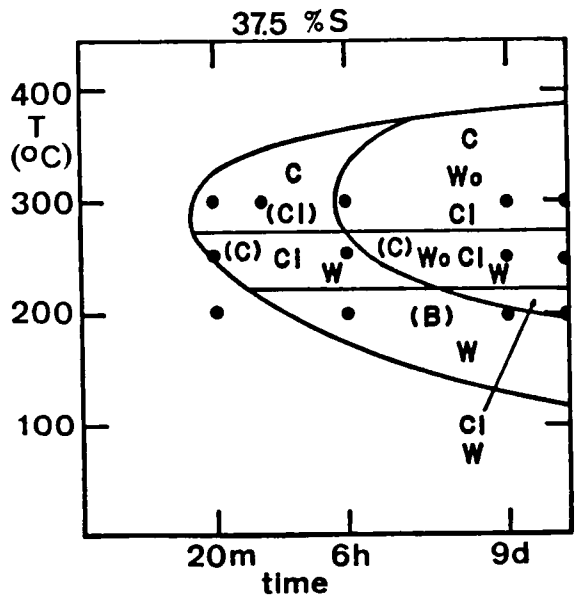

Figure 3.21. T-T-T (isopleth) diagram showing textural evolution in the mss-pn system; 20% ni join, 37.5% S. Dots: experimental points. Symbols are explained in the text.

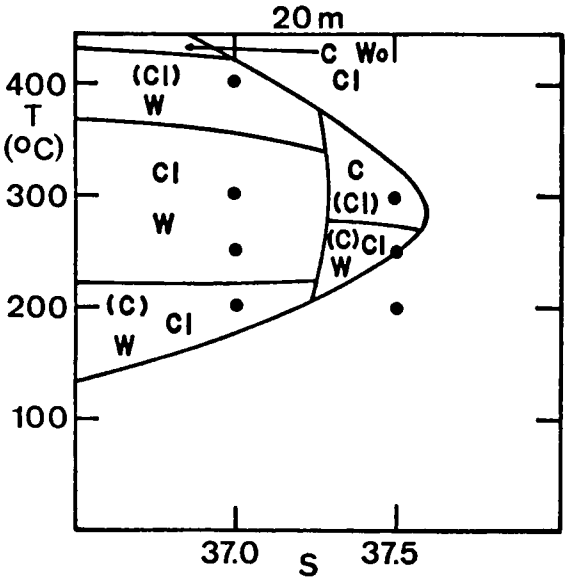

Figure 3.22. Isochronous diagram showing exsolution textures in the mss-pn system, 20% Ni join, 20-minute annealing. Dots: experimental points. Symbols are explained in the text.

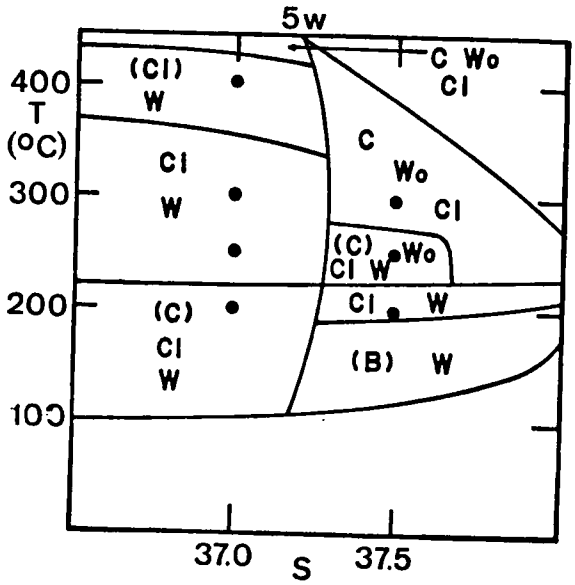

Figure 3.23. Isochronous diagram showing exsolution textures in the mss-pn system, 20% Ni join, 5-week annealing. Dots: experimental points. Symbols are explained in the text.

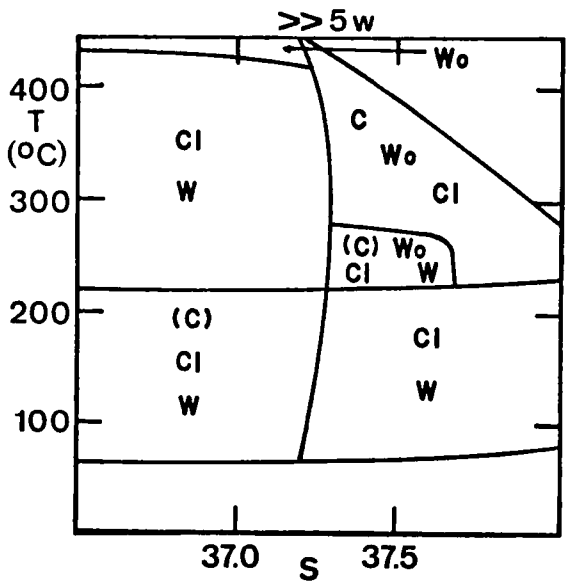

Figure 3.24. Exsolution textures predicted in the mss-pn system, 20% Ni join, after annealing times much greater than 5 weeks. Symbols are explained in the text.

1. C-forms are best developed at low degrees of supersaturation (i.e., in 37.5% charges) for any Ni content and all temperatures [Figures 3.1 (page 49), 3.16, and 3.21]. Charges with the lowest degree of supersaturation (i.e., 20% Ni, 37.0% S), on the other hand, contain virtually no C-forms (Figure 3.20). In general, C textures tend to yield Wo-forms by growth, partial breakdown, and coarsening, following the step C → Wo (Figure 3.25), as was shown for bn-cpy intergrowths, but seldom lose their shape completely.

2. P-forms are most abundant at low degrees of supersaturation and high temperatures (i.e., in charges with 6% Ni, 37.5% S annealed at 400° C, Figures 3.15 and 3.17). By contrast, they are virtually absent at the highest degree of supersaturation (20% Ni, 37.0% S) at any temperature (Figure 3.20).

3. B-forms are ubiquitous, except where P bodies are best developed, and are typically associated with short annealing times, usually less than 6 hours. Longer annealing produces Cl-forms, through growth and coarsening, following the step B → Cl.

4. W-forms are dominant at the highest degree of supersaturation (20% Ni, 37.0% S, Figure 3.20), and virtually absent at the lowest (6% Ni, 37.5% S, Figure 3.16). They are only partially developed between these extremes.

5. Cl-forms develop through coarsening of B-forms; therefore, they are found under the same conditions which promote the formation of the latter. Within this group, however, wedge-shaped bodies are most abundant in S-rich charges at relatively high temperatures (i.e., 300° and 250° C), while wire-shaped bodies are found at the highest degrees

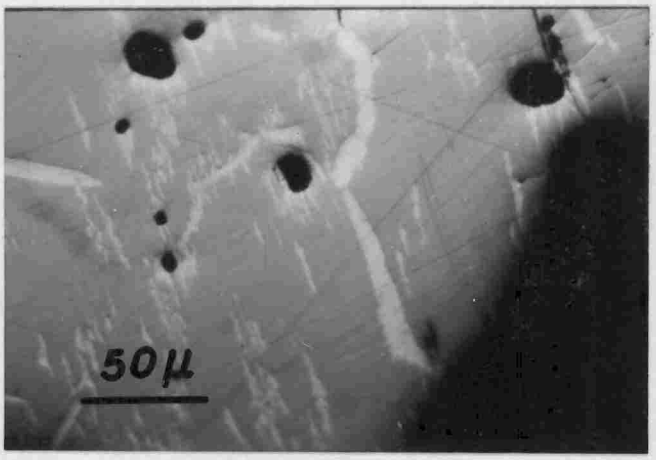

Figure 3.25. Cell texture breaking down and coarsening, and coarsened blades; 13% Ni, 37.5% S charge annealed 5 weeks at 250° C (gray: mss; white: pn).

of supersaturation (i.e., 20% Ni, 37.0% S), in association with W-forms.

6. Wo-forms typically derive from the evolution of C-forms. Therefore, they develop under the same conditions under which C-forms develop. In some cases, however, Wo-forms may develop through growth and coarsening of Cl and W-forms. Original P-forms may also grow and coarsen, yielding bodies which are morphologically undistinguishable from Wo-forms.

Interpretation of the Isothermal Experimental Textures

The development of po-pn experimental textures is tentatively explained on a thermodynamic and kinetic basis, as was done for the bornite-chalcopyrite intergrowths considered in the previous chapter. The observations made previously on the relationship between type of nucleation and growth on one hand, and the driving force responsible for exsolution as well as the values of the diffusivities on the other hand, still provide the basis for the interpretation which follows. Figures 3.26-3.27 and 3.28-3.29 constitute a simplified representation of Figures 3.17-3.19 and 3.22-3.24. They apply to dominant early and mature forms for 6 and 20% Ni charges respectively.

Early forms. As was noted previously, in the mss-pn system C-forms develop at low degrees of supersaturation, i.e., under conditions characterized by a relatively low driving force for exsolution (e.g.,

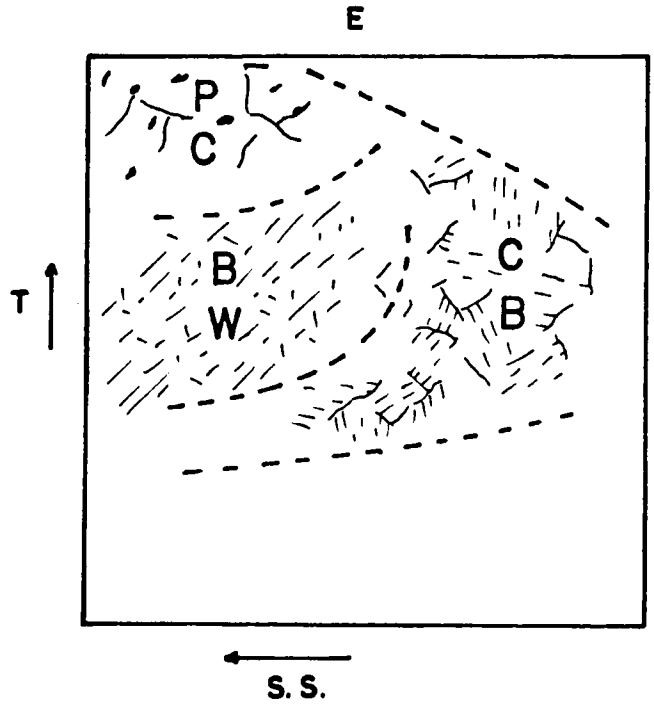

Figure 3.26. Schematic representation of early (E) exsolution textures in the mss-pn system; 6% Ni join. T: temperature; S.S.: degree of supersaturation.

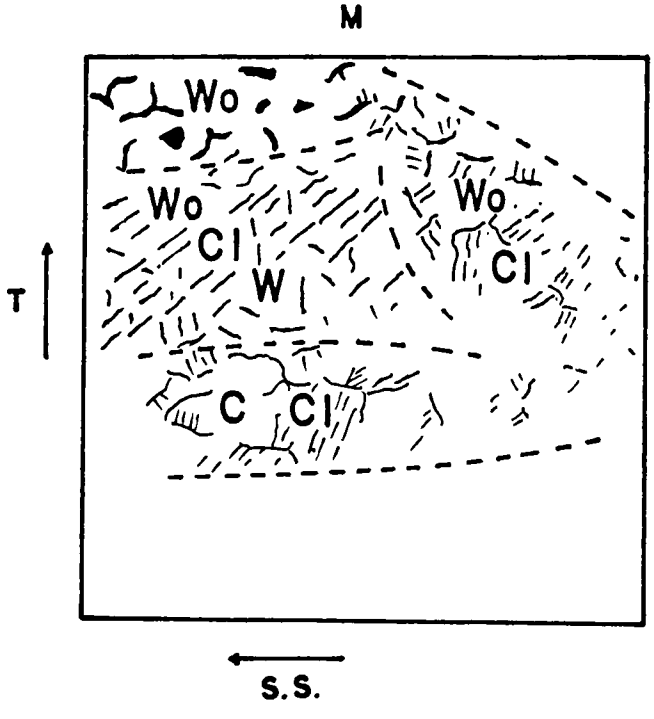

Figure 3.27. Schematic representation of mature (M) exsolution textures in the mss-pn system; 6% Ni join. T: temperature; S.S.: degree of supersaturation.

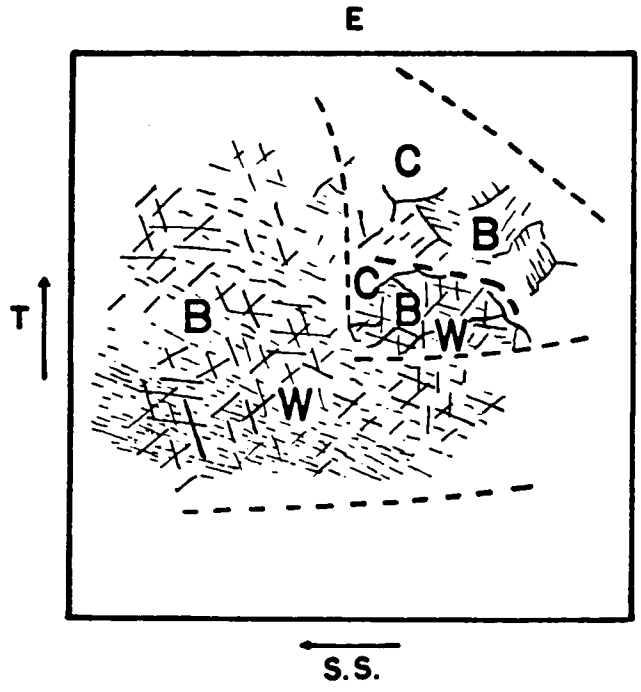

Figure 3.28. Schematic representation of early (E) exsolution textures in the mss-pn system; 20% Ni join. T: temperature; S.S.: degree of supersaturation.

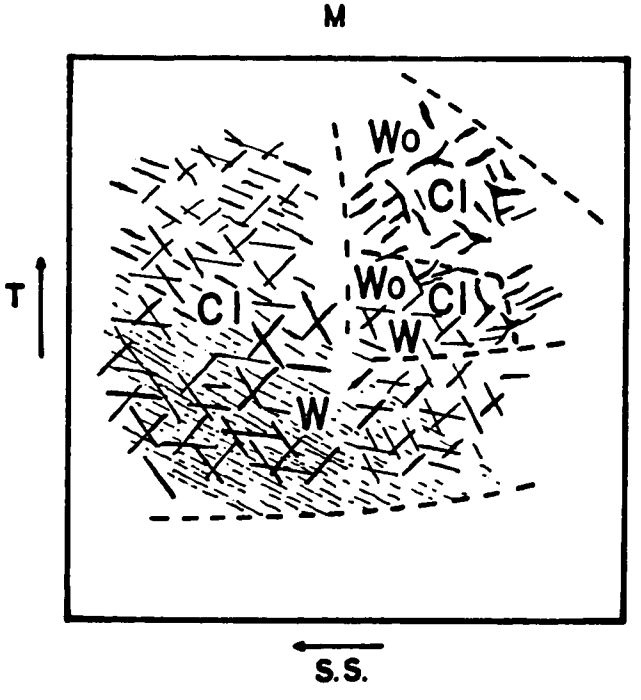

Figure 3.29. Schematic representation of mature (M) exsolution textures in the mss-pn system; 20% Ni join. T: temperature; S.S.: degree of supersaturation.

Yund and McCallister, 1970).[4] These conditions are compatible with nucleation and growth at high-energy sites such as grain boundaries, where the barrier against nucleation is low relative to that inside the matrix grains (see, for instance, Shewmon, 1969, and the discussion in the previous chapter). However, C-forms are also found at intermediate degrees of supersaturation, along with exsolution bodies inside the mss grains. For example, they coexist with Cl-forms in 6% Ni, 37.5% S charges annealed at 300° and 250° C for 5 weeks (Figure 3.18). This association indicates that nucleation and growth inside matrix grains need not preclude easier nucleation and growth along grain boundaries. For increasingly higher degrees of supersaturation, which for constant Ni compositions correspond to decreasing S contents, the relative importance of the former increases to a point where exsolution at grain boundaries is overshadowed by exsolution inside the grains. In particular, most 20% Ni, 37.0% S charges contain virtually no C-forms, but show dominant W and Cl-forms (Figure 3.20).

Such behavior seems to indicate gradual rather than discontinuous changes in the nucleation pattern associated with this system. In addition, the distribution of the textural forms which develop inside matrix grains (i.e., B and W) in relation to the initial degree of

---

[4]Due to the slanted nature of the solvus in the system under study (Figures 3.19 and 3.24), a decrease in temperature results in a substantial increase in the degree of supersaturation for a given composition. In the case of the bornite-chalcopyrite pseudo-binary system—in which the solvus is nearly vertical over the temperature range considered in the previous chapter—the degree of supersaturation is influenced mostly by compositional changes, and only to a limited extent by temperature variations for a given composition (Figure 2.1, page 8).

supersaturation suggests that W-forms require a higher driving force to develop than B-forms. In this case also, changes in the relative importance of B- and W-forms appear to be gradual. This can be observed by examining the textural fields within Figures 3.17, 3.18, and 3.26 for 6% Ni charges, and by comparing the textural assemblages of 20% Ni, 37.5% S charges annealed at 300° C with those annealed at 250° C for 5 weeks (Figure 3.23).

The exsolution patterns observed in the present experiments may be explained considering self-diffusion of Fe in pyrrhotites. Birchenall (1973) pointed out that both Fe and the slower S atoms diffuse about twice as fast parallel to the c axis as perpendicular to it in po. This applies to temperature above about 300° C, where po has the hexagonal structure of NiAs, and to temperatures as low as 250° where various superstructures along with monoclinic po may be present. For example, for $Fe_{0.93}S$, the Fe diffusivities (D_{Fe}) are 4.0×10^{-10} cm^2 sec^{-1} parallel to the c axis of po, and 1.8×10^{-10} cm^2 sec^{-1} normal to it at 413° C. For $Fe_{0.90}S$, D_{Fe} are 8.3×10^{-12} cm^2 sec^{-1} and 4.3×10^{-12} cm^2 sec^{-1} respectively at 296° C (Birchenall, 1973). The diffusivities of Ni in $Ni_{1-x}S$ show a similar pattern, and values close to those of Fe in po.

In a structural context, it appears that atom jumps in po most often take place between adjacent basal planes, i.e., from normal (octahedral) to interstitial (tetrahedral) sites, rather than between octahedral sites along the c axis, or along the same basal plane (Birchenall, 1973). Thus, diffusion rates in directions perpendicular and parallel to the c axis appear to be limited by the same type of

jump. This is consistent with the observation that the activation energies for diffusion are the same in both directions (Birchenall, 1973).

The B- and C1-forms obtained during the present experiments normally appear as en échelon linear bodies along one direction (Figures 3.4 and 3.11, pages 52 and 56), as do natural flames (Figure 1.3, page 4). However, optical observation reveals that these also appear as rosettes on (0001) sections of the mss matrix. Moreover, Francis et al. (1976) determined by precession studies that the (111) plane of platy pn bodies lies parallel to the (0001) plane of the matrix in po-pn intergrowths, and that there is a very close fit between the interatomic distances of the close-packed sulfur layers of pn along (111) and those of po along (0001).

These observations indicate that B1 and C1 bodies originate by nucleation and growth in a way compatible with the diffusion schemes discussed by Birchenall (1973). Thus, most atomic jumps lead to nucleation and growth of pn in directions parallel and perpendicular to the mss basal planes, but do not occur over large distances, producing planar en échelon bodies which appear as linear features along surfaces which are not parallel to the (0001) plane of the matrix.

The experimental W lamellae, typically straight and continuous, develop along either prismatic or pyramidal planes in the matrix. This deduction is based on the observation that they cross each other at 60° angles on the (0001) planes of mss. The possibility that they constitute prismatic planes is further supported by the work of Francis et al. (1976), who determined that the $(0\bar{1}1)$ and $(\bar{1}\bar{1}2)$ planes of

pn lie parallel to the $(11\bar{2}0)$ and $(10\bar{1}0)$ planes of po in po-pn intergrowths. The establishment of these textures involves nucleation and growth along planes either parallel to the c axis or inclined with respect to it, and long-range diffusion along the same directions. These processes seem to require a higher driving force than that responsible for the development of B- and Cl-forms, consistently with the observation by Birchenall (1973), that long-range diffusion may require a higher activation energy than short-range diffusion along the c direction. The same relationship may apply to long-range as opposed to short-range diffusion along mss basal planes, and would account for the presence of long, continuous wirey Cl bodies, rather than en échelon forms, at the highest degrees of supersaturation, in association with W-forms (Figures 3.6 and 3.10, pages 53 and 55).

P-forms are associated with subordinate C-forms at low degrees of supersaturation and high temperatures (i.e., 6% Ni, 37.5% S at 400° C, Figures 3.17 and 3.26, pages 59 and 65. Their predominance over C-forms is not easily explained on energetic grounds, i.e., by nucleation at 3- or 4-grain junctions, where the barrier to nucleation is smaller than at 2-grain junctions (Clemm and Fisher, 1955). Optical observation revealed that most holes, around which P-forms develop, are located inside matrix grains. It is suggested, therefore, that the nucleation barrier associated with holes is comparable to that of grain boundaries. Because of the high diffusivities prevailing at 400° C, however, holes may behave as point-like sinks which rapidly collect large numbers of Ni atoms from the surrounding matrix. The ensuing pn patches can thus reach dimensions that are large compared to the

thickness of C-bodies, which develop at grain boundaries. At lower temperatures, the lower diffusivities produce more even growth patterns, and a decrease in the relative importance of P-forms. This is evident, for instance, in 6% Ni, 37.5% S charges annealed at 300° and 250° C (Figure 3.17, page 59).

Mature forms. Mature forms develop through further growth and coarsening of early forms after much of the initial supersaturation in the matrix has disappeared as a result of exsolution. Therefore, they are controlled mainly by interfacial energy which, in turn, is influenced by the diffusivities of the atoms involved, i.e., by temperature (Greenwood, 1969). However, they are also influenced by the initial degree of supersaturation, being conditioned, in their development, by the early forms present.

While it is evident, from optical observations, that Cl-forms derive from B-forms and Wo-forms are coarsening products of Cl, W, and C-forms, it is also possible that some coarse forms may reflect the orientation of a section. For instance, it was pointed out that B- and Cl-forms are nearly tabular, and may appear as rosettes along basal sections of the mss matrix.

Comments on the Textural Development Model

The same observations made on the textural development model of Chapter II apply to the present model. First, they concern the nature of the boundary curves of Figures 3.15 through 3.24 (pages 58 through 61). Their position is not as definite as shown, since textural changes are gradual in nature. This is so because they are

controlled by interface and strain energy changes, which are 2 to 3 orders of magnitude smaller than the chemical free energy changes responsible for exsolution (e.g., Martin and Doherty, 1976). Secondly, and as a consequence of the above, mature forms evolving from early or other mature forms may not replace the latter completely—i.e., some early forms may survive and coexist with their coarsening products.

Thirdly, the location of the solvus lines above 250° C after 5 weeks and much longer times (Figures 3.18, 3.19, 3.23, and 3.24, pages 59 and 61) is based on the work of Naldrett et al. (1967). The existence and position of boundary curves separating the mss + pn from the mss field at low temperature after times much greater than 5 weeks (Figures 3.19 and 3.24) is based on the assumption that one phase only will be retained below about 80° C after very long annealing times, under metastable equilibrium conditions. It should be remembered, in this connection, that the low-temperature phase relations in the portion of the Fe-Ni-S system relevant to this study are not well understood (i.e., Misra and Fleet, 1973). For example, phases other than mss and pn may be part of stable assemblages at temperatures not far removed from 25° C, as is suggested by phase equilibria studies[5] and by the observation of natural assemblages, where po, pn, and pyrite coexist in apparent equilibrium.

---

[5]The mss field, continuous across the Fe-Ni-S system at temperatures above 992° C, breaks down between 400° and 300° C according to Misra and Fleet, 1973 (below 300° C according to Shewman and Clark, 1970, and Craig, 1973), producing mss of two compositions. Such a breakdown is of no concern here, since it affects areas, within the mss field, richer in Ni than any of the compositions used in the present experiments (Misra and Fleet, 1973; Craig, 1973).

Finally, although isothermal experiments do not duplicate natural conditions, they provide valuable information concerning the conditions under which given textures may form. The observation that the maximum annealing times of the experiments are short in a geologic context need not invalidate the applicability of the experimental results to situations involving slow cooling. For example, it can be predicted that during cooling from a homogeneous mss, C- and P-forms will develop first, and undergo substantial growth and coarsening, producing massive pn (Figures 3.27 and 3.29, pages 65 and 66). At lower temperatures (i.e., between 250° and 200° C), the lower diffusivities of both Fe and Ni may prevent re-equilibration, and produce higher degrees of supersaturation than were possible at higher temperatures. Under these conditions, linear features such as Cl or flames can develop. As metallurgical studies suggest, it may be expected that textural changes produced by cooling experiments will be shifted to lower temperatures and longer annealing times, as compared to identical changes occurring during isothermal experiments.

E. COOLING EXPERIMENTS AND GEOLOGIC IMPLICATIONS

In ore specimens, W textures involving po-pn are rare (Hawley and Haw, 1957). However, Ehrenberg (1932) reported examples of pn developed along three distinct directions in a po matrix. This paucity of occurrence is explainable, since W textures can only form at high degrees of supersaturation, as was determined in the present study. Most Sudbury-type deposits, on the other hand, develop into their final form through a series of chemical and textural re-equilibration steps,

which occur during very slow cooling from high temperatures (Craig et el., 1967; Naldrett et al., 1967; Naldrett, 1973). Such a condition is not compatible with high degrees of supersaturation, as was suggested by Durazzo and Taylor (1977).

In an attempt to reproduce the conditions under which Sudbury-type ore deposits re-equilibrate, experiments with controlled cooling rates were performed on charges of all five compositions used in the isothermal experiments (Table 3.1, page 48). The charges were cooled from 500°[6] to 100° C at 1° C/hour, and quenched in cold water (Appendix B, Table B.2). For one composition (6% Ni, 37.0% S), dissection experiments were conducted, i.e., different charges were quenched in cold water after they were cooled to 300°, 250°, 200°, and 150° C, in order to establish within which temperature range linear features such as B or Cl are best developed (Appendix B, Table B.3).

In all the five charges quenched at 100° C, pn segregations at grain boundaries, which evolve from early C textures, appeared extremely thick (Figure 3.12, page 56), as in natural specimens (Figure 3.14, page 56). Charges with the lower S content (37.0% S, both with 6 and 20% Ni), for which exsolution begins above 400° C, showed dominant, large Wo-forms, more abundant in the Ni-rich charge, and subordinate Cl-forms, similar to natural flames in places (Figure 3.13, page).

---

[6]At this temperature all the compositions of the present experiments plot within the mss field, above the solvus (Naldrett et al., 1967).

This relationship was reversed in the charges with a higher S content (i.e., 37.5% S, 6, 13, and 20% Ni), for which exsolution begins between 300° and 400° C. For these compositions, Cl-forms were dominant, with Wo-forms subordinate (Figure 3.12, page 56).

These results confirm the predictions, based on the isothermal experiments, that Wo-forms are favored when a low degree of supersaturation—always prevailing during slow cooling—is combined with a relatively high temperature for the beginning of exsolution. This is the case for compositions with the higher metal/sulfur ratio. When exsolution occurs at temperatures below about 250° C, lower values for the diffusivities may prevent as continuous a chemical re-equilibration as in the former case. As a result, a high enough degree of supersaturation may build up to produce en échelon linear features.

In the dissection experiments done on 37.0% S, 6% Ni charges, Wo-forms were dominant at all the temperatures at which the charges were quenched. However, only large, subordinate, wedge-like forms were present at 300° and 250° C. Their relative importance increased slightly at 200° C. At 150° C, Cl-forms with small, wavy terminations (i.e., $\leq$ 1 μm across) appeared, similar to natural flames in places. The increasing presence of small linear features at progressively lower temperatures reflects lower values for the diffusivities. It also indicates that pn flames, for which relatively little coarsening occurs, form at very low temperatures in nature. If the extremely slow cooling rates prevailing in natural environments are taken into account, such a temperature may be estimated at well below 200° C, perhaps even below 150° C.

The low atomic mobility prevailing at such temperatures may produce considerable strain at po-pn interfaces during the formation of flames. This would explain the "weak but distinct anisotropism" reported by Francis et al. (1976) in pn flames from specimens of the Creighton Mine (Sudbury).

It is important to emphasize that none of the cooling runs produced W textures.

The cooling experiments described above have considerable geologic significance because:

1. They produced textures which are remarkably similar to those observed in nature.

2. The textures obtained are consistent with the view (e.g., Hawley, 1962; Craig et al., 1967; Naldrett et al., 1967) that Ni sulfide deposits form at high temperature and undergo various re-equilibration steps during cooling.

3. The examination of experimental textures obtained by controlled cooling allows a partial reconstruction of the thermal history of Ni-sulfide deposits to be made. Specifically, the dissection cooling experiments indicate that coarse pn bodies, such as Wo, form at relatively high temperatures (i.e., above about 250° C), while coarsened linear features such as large Cl are indicative of exsolution at lower temperature (i.e., between approximately 250° and 150° C). Flames originate at even lower temperatures, possibly below 150° C.

F. CONCLUSIONS

The isothermal and the controlled cooling rate experiments performed during this investigation have provided a substantial contribution of data necessary for the interpretation of po-pn textures in Ni-sulfide deposits. More specifically, the isothermal experiments revealed how textural features are established and evolve in response to changes in the values of the relevant physico-chemical parameters.

For instance, it was determined that coarse, nonlinear features can develop at low degrees of supersaturation, while en échelon features along planes parallel to (0001) in mss require a higher driving force to develop than in the former case. W lamellae, observed along three crystallographic directions in the matrix, need a higher driving force yet to form. Their absence from natural Ni sulfide deposits is compatible with slow cooling, which does not promote high degrees of supersaturation.

The controlled cooling rate experiments represented an attempt to duplicate natural processes, despite the difference between the cooling rate of the experiments (1° c/hour) and the cooling rates which may prevail in nature. The ensuing textures contained fewer forms than those obtained isothermally, and appeared almost identical to those found in Ni-sulfide ores.

Both sets of experiments support the view held by many researchers that these types of deposits formed at high temperature, and assumed their present configuration through a number of re-equilibration steps. The dissection cooling rate experiments, in addition, allowed a temperature range to be assigned for the

establishment of the most significant textural forms of natural ores. Specifically, coarse, nonlinear pn forms can develop between 610° and around 250° C; coarsened linear features between 250° C and values as low as 150° C; flames at temperatures in the neighborhood of 150° C and, possibly, lower.

CHAPTER IV

SUMMARY AND CONCLUSIONS

The significance of textural features in sulfide mineral deposits is often unappreciated. Bornite-chalcopyrite (bn-cpy) and pyrrhotite-pentlandite (po-pn) intergrowths are widespread in copper and nickel sulfide mineral deposits. While past observational and experimental studies have failed to fully interpret their textures, they indicate that, in many cases, these develop through exsolution.

In order to better understand the influence of such factors as temperature, composition, and annealing time on exsolution textures, exsolution experiments were conducted in sealed, evacauated silica-glass tubes. The starting materials were bn-cpy and mss-pn solid solutions of various compositions, synthesized from high-purity elements and homogenized at high temperature. The former were annealed at temperatures between 250° and 100° C, and the latter at temperatures between 400° and 200° C, for varying amounts of time. All were examined in polished section under reflected light. Textural variations were described by T-T-T (isopleth) and isochronous diagrams, and interpreted in light of thermodynamic/kinetic considerations, and available diffusion data.

Additional experiments were performed in order to study the effect of heating on preexisting cpy lamellar forms in bn—a likely occurrence during metamorphism of Cu ores. In addition, homogeneous mss charges were cooled from 500° to 100° C at the rate of 1°/hour, in order

to observe the effect of slow cooling on mss-pn textures, since Ni-sulfide ores are considered, in general, to be high-temperature, magmatic deposits.

This investigation made a considerable contribution toward a better understanding of the factors controlling textural development in the bn-cpy and po-pn ststems. It was observed, in the first place, that for both systems considered, the initial degree of supersaturation and the diffusivities, both of which are functions of the temperature and composition, determine which textural types develop, through nucleation and growth, during the early stages of exsolution. The final textural configurations result from further growth and coarsening of the early product. Therefore, while strongly affected by temperature, textural evolution is also conditioned by the size and morphology of the early forms present.

During the isothermal experiments, the most common textures found in bn-cpy and po-pn natural intergrowths were reproduced. In addition, other forms were produced which are either uncommon or absent in ores, but provided useful—though indirect—information concerning the history of natural deposits.

In a strictly geologic context, the following points emerged:

1. Mutual boundary textures involving bn and cpy reflect prolonged exposure to temperatures above about 250° C. This is compatible with:

   a. Simultaneous precipitation above about 500° C.

   b. Exsolution during slow cooling from temperatures above the bn-cpy solvus.

   c. Metamorphism to temperatures near 250° C and above.

2. Intergrowths consisting of cpy Widmanstätten lamellae in a bn matrix are not easily explained as due to exsolution during slow cooling from temperatures above the solvus. Under these conditions, continuous re-equilibration would promote extremely low degrees of supersaturation, which favor cpy segregation at matrix grain boundaries. In addition, the thin Widmanstätten lamellae which can form at temperatures near 200° C, as the present experiments indicate, would probably be erased by coarsening during the long annealing times involved in slow cooling slightly below 200° C. Therefore, the processes which may account for the formation and retention of Widmanstätten textures involving bn and cpy include:

a. Low-temperature replacement.

b. Exsolution from anomalous bornites during heating to temperatures not exceeding 200°-250° C.

Anomalous bornites exist in nature, and their genesis has been explained experimentally.

3. The marked similarity between textures obtained by slow cooling of mss charges and natural po-pn intergrowths supports the view that most Ni-sulfide deposits formed at high temperature and re-equilibrated during slow cooling. In addition, the textures obtained by the mss-pn dissection experiments indicate that massive pn concentrations in ores develop between the upper stability limit of pn (i.e., 610° C) and approximately 250° C. Coarsened linear features are established at lower temperatures between about 250° and 150° C. Pn flames are probably formed around or slightly below 150° C.

BIBLIOGRAPHY

BIBLIOGRAPHY

F. M. Barrett, R. A. Binns, D. I. Groves, R. J. Marston, and K. G. McQueen (1973) Structural History and Metamorphic Modification of Archean Volcanic-Type Nickel Deposits, Yilgarn Block Western Australia. Econ. Geol., 72, 1195-1223.

P. B. Barton, Jr. (1970) Sulfide Petrology. MSA Spec. Paper 3, 187-198.

_____ (1972) Exsolution. In Encyclopedia of Geochemistry and Environmental Sciences IV A, R. Fairbridge, ed., 361-365. Van Nostrand Reinhold, N.Y.

P. B. Barton, Jr., and B. J. Skinner (1967) Sulfide Mineral Stabilities. In Geochemistry of Hydrothermal Ore Deposits, H. L. Barnes, ed. Holt, Rinehart and Winston, N.Y., 236-333.

P. B. Barton, Jr., and P. Toulmin, III (1961) Some Mechanisms for Cooling Hydrothermal Fluids. U.S.G.S., Prof. Paper 424-D, 348-352.

B. S. Bastin (1950) The Interpretation of Ore Textures. Geol. Soc. America Memoir 45.

C. E. Birchenall (1973) Diffusion in Sulfides. In Geochemical Transport and Kinetics, A. W. Giletti et al., ed., Carnegie Inst. Wash. Publ. 634, 53-59.

P. R. Brett (1962) Exsolution Textures and Rates in Solid Solutions Involving Bornite. Carnegie Inst. Wash. Year Book, 61, 155-157.

_____ (1963) The Cu-Fe-S System. Carnegie Inst. Wash. Year Book, 62, 193-196.

_____ (1964) Experimental Data from the System Cu-Fe-S and Their Bearing on Exsolution Textures in Ores. Econ. Geol., 59, 1241-1269.

_____ (1965) Kinetics of Exsolution in Two Sulfide Systems. Spec. Paper Geol. Soc. Am., 82, 18-19.

P. R. Brett, and R. A. Yund (1964) Sulfur-Rich Bornites. Am. Min., 49, 1084-1099.

L. J. Cabri (1973) New Data on Phase Relations in the Cu-Fe-S System. Econ. Geol., 68, 443-454.

J. W. Cahn (1956) The Kinetics of Grain Boundary Nucleated Reactions. Acta Met., 4, 449-459.

G. A. Chadwick (1972) Metallography of Phase Transformations. Butterworths, London.

J. H. Chen, and V. W. Harvey (1975) Cation Self-Diffusion in Chalcopyrite and Pyrite. Metall. Trans. B, 6, 331-339.

P. J. Clemm, and J. C. Fisher (1955) The Influence of Grain Boundaries on the Nucleation of Secondary Phases. Acta Met., 3, 70-73.

R. H. Condit, R. R. Hobbins, and C. E. Birchenall (1974) Self-Diffusion of Iron and Sulfur in Ferrous Sulfide. Oxid. Met., 8, 409-455.

J. R. Craig (1973) Pyrite-Pentlandite and Other Low-Temperature Relations in the Fe-Ni-S System. Am. J. Sci., 273-A, 496-510.

J. R. Craig, and G. Kullerud (1969) Phase Relations in the Cu-Fe-Ni-S System and Their Application to Magmatic Ore Deposits. In Magmatic Ore Deposits, H. D. B. Wilston, ed., Econ. Geol. Monogr. 4, 344-358.

J. R. Craig, A. J. Naldrett, and G. Kullerud (1967a) Succession of Mineral Assemblages in Pyrrhotite-Rich Ni-Cu Ores. Carnegie Inst. Wash. Year Book, 66, 431-434.

_____. 400° Isothermal Diagram (1967b) Carnegie Inst. Wash. Year Book, 66, 440-441.

A. Durazzo, and L. A. Taylor (1977) Experimental Textures in the Fe-Ni-S System. EOS, Trans. Am. Geoph. Union, 58, 519.

_____ (1978) Kinetic Factors in Bornite-Chalcopyrite Textural Developments. EOS, Trans. Am. Geoph. Union, 59, 396.

J. E. Dutrizac, R. J. C. MacDonald, and T. R. Ingraham (1970) The Kinetics of Dissolution of Bornite in Acidified Ferric Sulfate Solutions. Met. Trans., 1, 225-231.

A. B. Edwards (1954) Textures of the Ore Minerals and Their Significance. Australasian Inst. of Mining and Met., Melbourne.

H. Ehrenberg (1932) Orientierte Verwachsungen von Magnetkies und Pentlandit. Z. Kristallogr. 82, 309-315.

C. A. Francis, M. E. Fleet, K. C. Misra, and J. R. Craig (1976) Orientation of Exsolved Pentlandite and Synthetic Nickeliferous Pyrrhotite. Am. Min., 61, 913-920.

G. Frenzel (1959) Idait und "blaubleibender Covellin." Neues Jb. Miner. Abh., 93, 87-132.

K. von Gehlen (1963) Anomaler Bornit und seine Umbildung zu Idait und "Chalkopyrit" in deszendenten Kupfererzen von Sommerkahl (Spessart). Fortschr. Mineral., 41, 163.

M. N. Godlevskiy, A. P. Likhachev, N. G. Chuvikina, and A. D. Andronov (1971) Hydrothermal Synthesis of Pentlandite. Doklady Akad. Nauk SSSR-Miner., 196, 146-149.

M. Graterol, and A. J. Naldrett (1971) Mineralogy of the Marbridge No. 3 and No. 4 Nickel-Iron Sulfide Deposits. Econ. Geol., 66, 886-900.

G. W. Greenwood (1969) Particle Coarsening. In The Mechanism of Phase Transformations in Crystalline Solids. Monogr. and Rept. Series No. 33, Inst. of Metals, 103-110.

J. R. Gruner (1929) Structural Reasons for Oriented Intergrowths in Some Minerals. Am. Min., 14, 227-237.

J. E. Hawley (1962) The Sudbury Ores: Their Mineralogy and Origin. Can. Min., 7, 1-207.

J. E. Hawley, and V. A. Haw (1957) Intergrowths of Pentlandite and Pyrrhotite. Econ. Geol., 52, 132-139.

K. Koto, and N. Morimoto (1975) Superstructure Investigation of Bornite, Cu_5FeS_4 by Modified Partial Patterson Function. Acta Crystall. B31, 2268-2273.

G. Kullerud (1956) Subsolidus Phase Relations in the Fe-Ni-S System. Carnegie Inst. Wash. Year Book, 55, 175-180.

_____ (1963a) The Fe-Ni-S System. Carnegie Inst. Wash. Year Book, 62, 175-189.

_____ (1963b) Thermal Stability of Pentlandite. Can. Min., 7, 353-366.

_____ (1971) Experimental Techniques in Dry Sulfide Research. In Research Techniques for High Pressure and High Temperature, G. C. Ulmer, ed., Springer, Berlin, 288-315.

G. Kullerud, R. A. Yung, and G. H. Moh (1969) Phase Relations in the Cu-Fe-S, Cu-Ni-S and Fe-Ni-S System. In Magmatic Ore Deposits, H. D. B. Wilson, ed. Econ. Geol. Monogr. 4, 323-343.

A. D. Kurtz, B. L. Averbach, and M. Cohen (1955) Self-Diffusion of Gold in Gold-Nickel Alloys. Acta Metall., 3, 442-446.

D. Lundqvist (1947) X-Ray Studies on the Ternary System Fe-Ni-S. Ark. Kemi. Mineral. Geol. 24A, No. 22, 1947.

R. J. P. Lyon (1959) Time Aspects of Geothermometry. Mining Eng., 11, 1145-1151.

W. H. MacLean, L. J. Cabri, and J. E. Gill (1972) Exsolution Products in Heated Chalcopyrite. Can. J. Earth Sci., 9, 1305-1317.

J. W. Martin, and R. D. Doherty (1976) Stability of Microstructure in Metallic Systems. Cambridge Univ. Press, Cambridge.

K. C. Misra, and M. E. Fleet (1973) The Chemical Composition of Synthetic and Natural Pentlandite Assemblages. Econ. Geol., 68, 518-539.

N. Morimoto, J. W. Greig, and G. Tunnel (1960) Re-Examination of a Bornite from the Carn Brea Mine, Cornwall. Carnegie Inst. Wash. Year Book, 59, 122-126.

N. Morimoto, and G. Kullerud (1961) Polymorphism in Bornite. Am. Min., 46, 1270-1282.

F. R. N. Nabarro (1940) The Strains Produced by Precipitation in Alloys. Proc. Roy. Soc. (London), Ser. A, 175, 519-538.

A. J. Naldrett (1973) Nickel Sulfide Deposits—Their Classification and Genesis, with Special Emphasis on Deposits of Volcanic Association. CIM Trans., 76, 183-201.

A. J. Naldrett, J. R. Craig, and G. Kullerud (1967) The Central Portion of the Fe-Ni-S System and Its Bearing on Pentlandite Exsolution in Iron-Nickel Sulfide Ores. Econ. Geol., 62, 826-847.

A. J. Naldrett, and G. Kullerud (1966) Limits of the $Fe_{1-x}S$-$Ni_{1-x}S$ Solid Solution Between 600° and 250°. Carnegie Inst. Wash. Year Book, 65, 320-326.

_____ (1967) A Study of the Strathcona Mine and Its Bearing on the Origin of the Nickel-Copper Ores of the Sudbury District, Ontario. J. Petr., 8, 453-531.

W. H. Newhouse (1928) The Microscopic Criteria of Replacement in the Opaque Ore Minerals. In The Laboratory Investigation of Ores, E. E. Fairbanks, ed., McGraw-Hill, New York, 147-161.

E. R. Phillips (1974) Myrmekite—One Hundred Years Later. Lithos, 7, 181-194.

J. Prouvost (1960) Remarques sur la Composition et le Pouvoir Reflecteur de la Bornite (Cu_5FeS_4). Comp. Rend. Congres Soc. Savantes, Sect. Sci., Dijon, 1959, 365-372.

A. Putnis (1978) Talnakhite and Mooihoekite: The Accessibility of Ordered Structures in the Metal-Rich Region Around Chalcopyrite. Can. Min., 16, 23-30.

P. Ramdohr (1969) The Ore Minerals and Their Intergrowths. Pergamon Press, Oxford

J. R. Ray (1930) Synthetic Sulfide Replacement of Ore Minerals. Econ. Geol., 25, 433-451.

W. M. B. Roberts (1963) The Low Temperature Synthesis in Aqueous Solution of Chalcopyrite and Bornite. Econ. Geol., 58, 52-61.

W. Rostoker, and J. Dvorak (1977) Interpretation of Metallographic Structures. 2nd ed., Academic Press, N.Y.

G. I. Samal, and M. P. Gilevich (1978) Self-Diffusion of Copper in Bornite and Chalcopyrite. Vestsi Akad. Navuk BSSR, Ser. Khim. Navuk, 1, 126-129.

H. Schneiderhöhn (1952) Erzmikroskopisches Praktikum. E. Schweizerbart'sche Verlagsbuchhandlung, Stuttgart.

C. Schouten (1934) Structures and Textures of Synthetic Replacements in "Open Space." Econ. Geol., 29, 611-658.

G. M. Schwartz (1931a) Intergrowth of Bornite and Chalcopyrite. Econ. Geol., 26, 186-201.

_____ (1931b) Textures Due to Unmixing of Solid Solutions. Econ. Geol., 26, 739-763.

_____ (1951) Classification and Definitions of Textures and Mineral Structures in Ores. Econ. Geol., 46, 578-591.

R. W. Shewman, and L. A. Clark (1970) Pentlandite Phase Relations in the Fe-Ni-S System and Notes on the Monosulfide Solid Solution. Can. J. Earth Sci., 7, 67-85.

P. G. Shewmon (1969) Transformations in Metals. McGraw-Hill, N.Y.

R. M. Sillitoe, and A. M. Clark (1969) Copper and Copper-Iron Sulfides as the Initial Products of Supergene Oxidation, Copiapo Mining District, Northern Chile. Am. Min., 54, 1684-1710.

N. D. Sindeeva (1964) Mineralogy and Types of Deposits of Selenium and Tellurium. Interscience, N.Y.

R. L. Stanton (1972) Ore Petrology. McGraw-Hill, N.Y.

R. L. Stanton, and H. Gorman (1968) A Phenomenological Study of Grain Boundary Migration in Some Common Sulfides. Econ. Geol. 63, 907-923.

A. Sugaki (1951a) Thermal Experiments on the Lattice Intergrowth of Chalcopyrite and Klaprothite in Bornite from the Obari Mine, Japan. Sci. Repts. Tohoku Univ., Ser. III, 4 (1), 11-17.

_____ (1951b) Thermal Studies on the Lattice Intergrowths of Chalcopyrite in Bornite from the Akayama Mine, Japan. Sci. Repts. Tohoku Univ., Ser. III, 4 (1), 19-28.

A. Sugaki (1955) Thermal Studies on the Lattice Intergrowths of Chalcopyrite in Bornite from the Jinmu Mine, Japan. Sci. Repts. Tohoku Univ., Ser. III, 5 (1), 113-128.

_____ (1965) Studies on the Join Cu_5FeS_4-$CuFeS_{2-x}$ as Geothermometer. Journ. Japan Assoc. Min. Petr. Econ. Geol., 53, (1), 1-17.

T. Takeuchi, and M. Nambu (1956) On the Genesis of the Chalcopyrite Lattice in Bornite. Sci. Repts. Tohoku Univ., Ser. A, 8, 31-44.

L. A. Taylor (1971) The Fe-S-O System: Oxidation of Pyrrhotites and the Formation of Anomalous Pyrrhotite. Carnegie Inst. Wash. Year Book, 70, 287-290.

W. Tufar (1967) Der Bornit von Trattenbach (Niederösterreich). N. Jb. Miner. Abh., 106, 334-351.

R. W. Van Der Veen (1925) Mineragraphy and Ore Deposition. G. Naeff, The Hague.

L. H. Van Vlack (1965) Microstructures. In Physical Metallurgy, R. W. Cahn, ed., John Wiley and Sons, N.Y.

J. D. Verhoeven (1975) Fundamentals of Physical Metallurgy. John Wiley and Sons, New York.

A. Wandke (1926) Molecular Migration and Mineral Transformation. Econ. Geol., 28, 166-171.

R. A. Yung, and H. T. Hall (1970) Kinetics and Mechanism of Pyrite Exsolution from Pyrrhotite. J. Petrology, 11, 381-404.

R. A. Yung, and R. H. McCallister (1970) Kinetics and Mechanisms of Exsolution. Chem. Geol., 6, 5-30.

T. O. Ziebold, and R. E. Ogilvie (1963) Quantitative Analysis with the Electron Microanalyzer. Analyt. Chem., 35, 621-627.

APPENDIXES

APPENDIX A

EXPERIMENTS WITHIN THE BN-CPY SYSTEM

Table A.1

Summary of the Annealing Experiments Involving cpy Exsolution from bn-cpy Solid Solutions of Various Compositions

Composition (Mole %)	Annealing Temperature (°C)	Annealing Time	Textural Forms[a]
94bn-6cpy	250	20 minutes	(P) C Wo
		1 hour	(P) C Wo
		1 day	C Wo
		5 days	Wo
		3 weeks	(C) Wo
	200	1 hour	C W Em
		1 day	C (W) Em
		5 days	(P) C (W) Wo Em
		3 weeks	C (W) Wo Em
		6 weeks	C W Wo Em
	150[b]	1 hour	no exsln
		1 day	C W Em
		5 days	C
		3 weeks	C W Em (Wo)
		10 weeks	C Wo W Em
	100[b]	1 day	no exsln
		5 days	C Em
		3 weeks	C W Em
		10 weeks	C Wo W Em
88bn-12cpy	250	20 minutes	(P) C W Em
		1 hour	(P) C W Em
		6 hours	(P) C Wo W Em
		1 day	C Wo
		4 days	C Wo
		2 weeks	(C) Wo
	200	1 hour	C W Em
		6 hours	(P) C W Em
		1 day	C W Em
		5 days	C (Wo) W Em
		3 weeks	C Wo W Em
		6 weeks	C Wo W Em
	150	6 hours	(C) W Em
		1 day	C W Em
		5 days	C W Em
		3 weeks	C W Em
		6 weeks	(C) W Em
		10 weeks	C (Wo) W Em

Table A.1 (continued)

Composition (Mole %)	Annealing Temperature (°C)	Annealing Time	Textural Forms[a]
	100	12 hours	(W) (Em)
		2 days	(C) W Em
		1 week	(C) W (Em)
		4 weeks	C W Em
		10 weeks	(C) (Wo) W Em
88bn-12cpy[c]	250	20 minutes	(PI C W Em
		1 hour	(P) C (Wo) W Em
		6 hours	(P) C Wo W Em
		1 day	C Wo W Em
		4 days	C Wo W Em
		2 weeks	(C) Wo (W) (Em)
	200	1 hour	C W Em
		6 hours	(P) C (Wo) W Em
		1 day	(P) C Wo W Em
		5 days	C Wo W Em
		3 weeks	C Wo W Em
		6 weeks	C Wo W Em
	150	6 hours	(C) W Em
		1 day	C W Em
		5 days	C W Em
		3 weeks	C W Em
		6 weeks	C W Em
		10 weeks	C (Wo) W Em
	100	12 hours	(Em)
		2 days	W (Em)
		1 week	C
		4 weeks	C W Em
		10 weeks	C (Wo) W (Em)
75bn-25cpy	250	20 minutes	(P) Wo
		1 hour	Wo
		6 hours	Wo
		1 day	Wo
		4 days	Wo
	200	20 minutes	P
		1 hour	P (Wo)
		6 hours	(P) Wo
		1 day	Wo
		4 days	Wo
		2 weeks	Wo

Table A.1 (continued)

Composition (Mole %)	Annealing Temperature (°C)	Annealing Time	Textural Forms[a]
	150	20 minutes	(W)
		1 hour	W
		6 hours	W (Em)
		1 day	W (Wo)
		4 days	W (Wo)
		2 weeks	W (Wo)
		8 weeks	W (Wo)
	100	12 hours	no exsln
		2 days	W
		1 week	W (Em)
		4 weeks	W (Wo)
		10 weeks	W (Wo)

[a]C = Cell; P = Patches; W = Widmanstätten; Wo = Worms; Em = Emulsion; bn = Bornite; cpy = Chalcopyrite. Textural symbols are defined in the text. Parentheses around textural symbols indicate that the corresponding textural forms are subordinate.

[b]These charges contain minor amounts of a bluish phase, probably digenite.

[c]Doped with 500 ppm Se.

Table A.2

Summary of the Annealing Experiments Performed on W Textures Formed on Quenching from 800° C, Following 1 Week Subsequent Annealing at 150° C

Composition (Mole %)	Annealing Temperature (°C)	Annealing Time	Textural Forms[a]
30bn-70cpy	200	4 weeks	(C), large W, (small W)
	250	4 weeks	C, Wo, large W, (small W)
	300	4 weeks	C, Wo, large W, small W
	350	4 weeks	(C), Wo, (large W), small W

[a]C = Cell; P = Patches; W = Widmanstätten; Wo = Worms; Em = Emulsion; bn = Bornite; cpy = Chalcopyrite. Textural symbols are defined in the text. Parentheses around textural symbols indicate that the corresponding textural forms are subordinate.

APPENDIX B

EXPERIMENTS WITHIN THE MSS-PN SYSTEM

Table B.1

Summary of the Annealing Experiments Involving pn Exsolution from Monosulfide Solid Solutions (mss) of Various Compositions

Composition (Weight %)			Annealing Temperature (°C)	Annealing Time	Textural Forms[a]
Fe	Ni	S			
57.0	6.0	37.0	400	20 minutes	P (C)
				1 hour	P (C) (B)
				6 hours	(P) C (Cl)
				36 hours	Wo C Cl
				9 days	Wo (C) Cl
				5 weeks	Wo (C) Cl
			300	20 minutes	(P) (C) Cl (W)
				1 hour	(P) (C) Cl (Wo) W
				6 hours	(P) (C) Cl (Wo) W
				9 days	(P) (C) Cl Wo W
				5 weeks	(P) (C) Cl Wo W
			250	20 minutes	(C) (Cl)
				6 hours	(C) Cl (Wo) W
				9 days	C Cl Wo W
				5 weeks	C Cl Wo W
			200	20 minutes	no exsln
				6 hours	C Cl (Wo) W)
				9 days	C Cl (Wo) (W)
				5 weeks	C Cl Wo (W)
56.5	6.0	37.5	300	20 minutes	(P) (B)
				1 hour	(P) (C) (B)
				6 hours	(P) C Cl (Wo)
				9 days	(P) C Cl Wo
				5 weeks	(P) C Cl Wo
			250	20 minutes	no exsln
				6 hours	C B Cl
				9 days	C Cl Wo
				5 weeks	C Cl Wo
			200	20 minutes	no exsln
				6 hours	(C) (B)
				9 days	C (B) Cl (W)
				5 weeks	C (B) Cl (W)

Table B.1 (continued)

Composition (Weight %)			Annealing Temperature (°C)	Annealing Time	Textural Forms[a]
Fe	Ni	S			
49.5	13.0	37.5	300	20 minutes	(P) C B
				1 hour	(P) C (B) Cl (Wo)
				6 hours	(P) C Cl Wo
				9 days	(P) C Cl Wo
				5 weeks	(P) C Cl Wo
			250	20 minutes	C (B)
				6 hours	C Cl (W)
				9 days	C Wo Cl (W)
				5 weeks	C Wo Cl (W)
			200	20 minutes	no exsln
				6 hours	C (B)
				9 days	C Cl Wo W
				5 weeks	C Cl Wo W
43.0	20.0	37.0	400	20 minutes	(Cl) W
				1 hour	(Cl) W
				6 hours	(Cl) W
				36 hours	(Cl) W
				9 days	(Cl) W
				5 weeks	(Cl) W
			300	20 minutes	Cl W
				1 hour	Cl W
				6 hours	Cl W
				9 days	Cl W
				5 weeks	Cl W
			250	20 minutes	Cl W
				6 hours	Cl W
				9 days	Cl W
				5 weeks	Cl W
			200	20 minutes	(C) Cl W
				6 hours	(C) Cl W
				9 days	(C) Cl W
				5 weeks	Cl W
42.5	20.0	37.5	300	20 minutes	C Cl
				1 hour	C Cl (Wo)
				6 hours	(C) Cl Wo
				9 days	C Cl Wo
				5 weeks	C Cl Wo

Table B.1 (continued)

Composition (Weight %)	Annealing Temperature (°C)	Annealing Time	Textural Forms[a]
	250	20 minutes	(C) W
		6 hours	(C) Cl W
		9 days	Cl Wo W
		5 weeks	(C) Cl Wo W
	200	20 minutes	no exsln
		6 hours	(B) W
		9 days	(B) (Cl) W
		5 weeks	(B) Cl W

[a]C = Cells; P = Patches; B = Blades; W = Widmanstätten; Wo = Worms; Cl = Coarsened linear; mss = Monosulfide solid solution; pn = Pentlandite. Textural symbols are defined in the text. Parentheses around textural symbols indicate that the corresponding textural forms are subordinate.

Table B.2

Experiments Involving Cooling of Homogeneous Mss from 500° to 100° C at 1° C/Hour, and Quenching in Cold Water from 100° C

Composition (Weight %)			Textural Forms[a]
Fe	Ni	S	
57.0	6.0	37.0	Dominant large Wo, abundant large Cl, minor flames
56.5	6.0	37.5	Large Wo, dominant large Cl, minor flames
49.5	13.0	37.5	Large Wo, dominant large Cl, flames
43.0	20.0	37.0	Dominant large Wo, abundant large Cl, flames
42.5	20.0	37.5	Large Wo, dominant large Cl, flames

[a]C = Cells; P = Patches; B = Blades; W = Widmanstätten; Wo = Worms; Cl = Coarsened linear; mss = Monosulfide solid solutions; pn = Pentlandite. Textural symbols are defined in the text. Parentheses around textural symbols indicate that the corresponding textural forms are subordinate.

Table B.3

Experiments Involving Cooling of Homogeneous Mss from 500° C to 1° C/Hour, and Quenching in Cold Water from Various Temperatures. The Composition of All Experiments is (Weight %): 57.0 Fe, 6.0 Ni, 37.0 S

Temperature from which Charges were Quenched (°C)	Textural Forms[a]
300	Dominant large Wo, large Cl
250	Dominant large Wo, large Cl
200	Dominant large Wo, more abundant large Cl
150	Dominant large Wo, abundant large Cl, minor flames

[a]C = Cells; P = Patches; B = Blades; W = Widmanstätten; Wo = Worms; Cl = Coarsened linear; mss = Monosulfide solid solution; pn = Pentlandite. Textural symbols are defined in the text. Parentheses around textural symbols indicate that the corresponding textural forms are subordinate.

VITA

Aldo Durazzo was born in Rome, Italy, on September 1, 1936. Following graduation from high school, he enrolled at the University of Rome and received a degree in Geological Sciences in 1961. After being awarded a Fulbright Travel Grant, he attended the Pennsylvania State University as a graduate assistant and received a Master's degree in Mineral Economics in 1966.

During the following years he worked as a mining geologist for the Mufulira Copper Mines Ltd. in Zambia (1967-68) and as head of the Geology Department for Tarkwa Goldfields in Ghana (1969-70). In 1970, he joined the Mining Journal of London, serving as mining editor until 1972, when he returned to Italy to work as a geologic consultant.

In 1973, he became a faculty member at the University of Camerino, where he taught Petrology and Applied Geology until 1974, when he enrolled at The University of Tennessee Graduate School on a Ph.D. program in Geological Sciences. He interrupted his graduate program in 1979 in order to rejoin the University of Camerino, teaching Petrology for the academic year 1979-80, and doing petrological research at the University of Rome. He returned to The University of Tennessee in the summer of 1980 to complete the Doctor of Philosophy degree.